Identification of Doping Profiles in Semiconductor Devices

Martin Burger*, Heinz W. Engl*, Peter A. Markowich†, Paola Pietra‡

Abstract

This paper is devoted to the identification of doping profiles in the stationary drift-diffusion equations modeling carrier and charge transport in semiconductor devices. We develop a framework for these *inverse doping problems* with different possible measurements and discuss mathematical properties of the inverse problem, such as the identifiability and the type of ill-posedness.

In addition, we investigate scaling limits of the drift-diffusion equations, where the inverse doping problem reduces to classical (elliptic) inverse problems. As a first concrete application we consider the identification of piecewise constant doping profiles in p-n diodes.

Finally, we discuss the stable solution of the inverse doping problem by regularization methods and their numerical implementation. The theoretical statements are tested in a numerical example for a p-n diode.

1 Introduction

Over the last decades, semiconductor devices have played a fundamental role in modern electronics. Together with their manufacturing, their mathematical modeling has developed well, since the 1950s, when Van Roosbroeck (cf.[51]) first formulated the fundamental semiconductor device equations, which will be presented in Section 2. Detailed expositions concerning the modeling, analysis and simulation of semiconductor devices can be found in the monographs [38, 40, 44].

Recently, there has been a growing interest in mathematical methods for designing devices in an optimal way with respect to several criteria (cf. e.g. [29, 47, 48]) and in identifying relevant material properties (cf. [14, 21, 22, 23]). The quantity to be identified or optimized is the *doping profile*, which is the density difference of ionized donors and acceptors. In the most frequently applied doping technique of silicon devices, *ion implantation*, it is only possible to obtain a rough estimate of the doping profile by process modeling (cf. e.g. [44] for further details). In order to determine the real doping profile, reconstruction methods from indirect data have to be used.

A well-investigated approach to obtain data for the identification is the technique of laser beam induced currents, where measurements of the mean contact current are available for arbitrary generation sources (the so-called LBIC image). The identification of doping-profiles from the LBIC-image has been investigated by Fang and Ito (cf. [22, 23]), who verified the identifiability and developed an algorithm for the numerical solution.

*Institut für Industriemathematik, Johannes Kepler Universität Linz, Altenbergerstr. 69, A-4040 Linz, Austria.

†Institut für Mathematik, Universität Wien, Boltzmanngasse 9 A-1090 Vienna, Austria

‡Istituto di Analisi Numerica del C.N.R., Via Ferrata 1, I-27100 Pavia, Italy

However, for technological reasons and for convenience one often has to use different measurements than the LBIC-technique. In this paper we shall investigate two important inverse problems, namely the identification of the doping profile from measurements of the *voltage-current map* and from *capacitance measurements.* The voltage-current map links the applied voltage on the contacts to the output current in normal direction on a part of the contacts, close to equilibrium (zero applied voltage) it can be defined as a one-to-one mapping. The capacitance is the variation of the electrical field in normal direction on a part of the contact with respect to the applied voltage. For the sake of simplicity we restrict our attention to the variation around equilibrium. We shall call the identification of doping profiles from such indirect measurements *inverse doping problems.*

Besides the different types of data we shall also treat some important limiting cases, which arise from the original problem as asymptotics for certain parameters tending to zero such as the so-called case of *zero space charge* or the *unipolar drift-diffusion equations.* In addition, we shall investigate an interesting special case for a $P-N$-diode, where the doping profile is assumed a-priori to be a piecewise constant function. The quantity to be identified in this application is the jump between the two regions, in which the doping profile is constant, the so-called *P-N junction.*

The paper is organized as follows. In Section 2 we review the stationary drift-diffusion equations and its basic properties. The *inverse doping problems* for the drift-diffusion equations are presented in Section 3, where we also discuss the mathematical structures corresponding to certain kinds of data and analyze associated operators as well as the corresponding parameter-to-output maps.

Section 4 is devoted to the question of identifiability, which is treated in a special case, namely unipolarity. This allows us to develop very strong analogies to the well-known technique of electrical impedance tomography and to carry over corresponding uniqueness results.

In Section 5 we investigate another interesting special case, namely the identification of a piecewise constant doping profile in a p-n diode. Although this problem can be interpreted as a special case of reconstructing a general doping profile, it has many special features that require a specific treatment. In particular we can consider a smaller set of data for this subproblem, since we have restricted the shape of the doping profile. The main feature of this inverse problem becomes the reconstruction of the curve that marks the discontinuity of the profile, a problem which is rather related to so-called *inverse boundary problems* (cf. e.g. [3, 5, 10]) or the *inverse conductivity problem with one measurement* (cf. e.g. [24, 35, 4]). Indeed, scaling limits of the drift-diffusion equations will lead exactly to such problems.

Due to the instability of the inverse doping problem, regularization methods have to be used to obtain stable approximations of the solution, which will be discussed in Section 6. We focus on iterative regularization methods, which we briefly review and discuss with respect to typical features in the application to the inverse doping problem. One of these features is the most-likely *exponential ill-posedness* of the problem, which enforces a special treatment in the convergence analysis and influences strongly the rate of convergence we may expect. Another aspect of the inverse doping problem is its large scale, which enforces to pay particular attention to the efficiency of the methods used for its numerical solution.

In a numerical example concerned with a p-n diode, we test the behavior of the Landweber iteration for the inverse doping problem in Section 7. Finally, we present conclusions and give a perspective on future work in Section 8.

2 The Stationary Drift-Diffusion Equations

The stationary drift-diffusion equations are a coupled system of nonlinear partial differential equations for the electrostatic potential V, the electron density n and the hole density p

$$\begin{aligned}
\operatorname{div}(\epsilon_s \nabla V) &= q(n-p-C) && \text{in } \Omega && \text{(Poisson equation)}\\
\operatorname{div}(D_n \nabla n - \mu_n n \nabla V) &= R && \text{in } \Omega && \text{(electron continuity equation)}\\
\operatorname{div}(D_p \nabla p + \mu_p p \nabla V) &= R && \text{in } \Omega && \text{(hole continuity equation)},
\end{aligned}$$

where the domain $\Omega \subset \mathbf{R}^d$ $(d = 1, 2, 3)$ represents the semiconductor device. Here ϵ_s denotes the semiconductor permittivity, q the elementary charge, μ_n and μ_p are the electron and hole mobility, D_n and D_p are the electron and hole diffusion coefficients. R denotes the *recombination-generation rate*, which generally depends on n and p. We assume that R is of the standard form

$$R = F(n,p,x)(np - n_i^2), \tag{2.1}$$

where F is a nonnegative smooth function, which holds e.g. for the frequently used *Shockley-Read-Hall* rate

$$R_{SRH} = \frac{np - n_i^2}{\tau_p(n+n_i) + \tau_n(p+n_i)}$$

or the *Auger recombination-generation rate*

$$R_{AU} = (C_n n + C_p p)(np - n_i^2).$$

This system is supplemented by homogeneous Neumann boundary conditions on a part $\partial\Omega_N$ (open in $\partial\Omega$) of the boundary. On the remaining part $\partial\Omega_D$ (with positive $(d-1)$-dimensional Lebesgue-measure), the following Dirichlet conditions are imposed:

$$\begin{aligned}
V(x) &= V_D(x) = U(x) + V_{bi}(x) = U(x) + U_T \ln\left(\frac{n_D(x)}{n_i}\right) && \text{on } \partial\Omega_D\\
n(x) &= n_D(x) = \frac{1}{2}\left(C(x) + \sqrt{C(x)^2 + 4n_i^2}\right) && \text{on } \partial\Omega_D\\
p(x) &= p_D(x) = \frac{1}{2}\left(-C(x) + \sqrt{C(x)^2 + 4n_i^2}\right) && \text{on } \partial\Omega_D,
\end{aligned}$$

where n_i is the intrinsic carrier density, U_T the thermal voltage and U is the applied potential.

A standard assumption about the mobilities and diffusion coefficients are the Einstein relations:

$$D_n = \mu_n U_T, \qquad D_p = \mu_p U_T, \tag{2.2}$$

which enables the transformation into the so-called *Slotboom variables* u and v defined by

$$n = C_0 \delta^2 e^{V/U_T} u, \qquad p = C_0 \delta^2 e^{-V/U_T} v, \tag{2.3}$$

where $\delta^2 = \frac{n_i}{C_0}$ with a typical value C_0 for the doping profile, which is also scaled by C_0. In order to obtain a completely dimensionless system, we use the scaled length $\frac{x}{L}$, where L is a typical length for the device and replace the mobilities by

$$\tilde{\mu}_n = \frac{U_T}{L}\mu_n \qquad \text{and} \qquad \tilde{\mu}_p = \frac{U_T}{L}\mu_p.$$

The assumptions that ϵ_s is constant and the rescaling of the potential to $\frac{V}{U_T}$ now yield the system

$$\lambda^2 \Delta V = \delta^2(e^V u - e^{-V} v) - C \quad \text{in } \Omega \tag{2.4}$$
$$\operatorname{div} J_n = \delta^4 Q(u,v,V,x)(uv-1) \quad \text{in } \Omega \tag{2.5}$$
$$\operatorname{div} J_p = -\delta^4 Q(u,v,V,x)(uv-1) \quad \text{in } \Omega \tag{2.6}$$
$$J_n = \tilde{\mu}_n \delta^2 e^V \nabla u \quad \text{in } \Omega \tag{2.7}$$
$$J_p = -\tilde{\mu}_p \delta^2 e^{-V} \nabla v \quad \text{in } \Omega \tag{2.8}$$

where $\lambda^2 = \frac{\epsilon_s U_T}{q C_0 L^2}$ and Q is defined via the relation $F(n,p,x) = Q(u,v,V,x)$. The new variables J_n and J_p are the scaled electron and hole current densities; the above mixed formulation seems to be natural for cases where one is interested in these quantities, since it contains them explicitly. In addition, the mixed formulation has advantages for the construction of numerical methods to solve the drift-diffusion equations and to determine the current densities (cf. [8] for further details). Unless specified otherwise, we shall set δ to 1 and write again $\mu_{n/p}$ instead of $\tilde{\mu}_{n/p}$ in the sequel.

The Dirichlet boundary conditions can be written as

$$V = U + V_{bi} = U + \ln\left(\frac{1}{2\delta^2}(C + \sqrt{C^2 + 4\delta^2})\right) \quad \text{on } \partial\Omega_D \tag{2.9}$$
$$u = e^{-U} \quad \text{on } \partial\Omega_D \tag{2.10}$$
$$v = e^{U} \quad \text{on } \partial\Omega_D. \tag{2.11}$$

On the remaining part $\partial\Omega_N = \partial\Omega - \partial\Omega_D$, the homogeneous Neumann conditions can be formulated in terms of J_n and J_p, i.e.,

$$\frac{\partial V}{\partial \nu} = 0 \quad \text{on } \partial\Omega_N \tag{2.12}$$
$$J_n.\nu = 0 \quad \text{on } \partial\Omega_N \tag{2.13}$$
$$J_p.\nu = 0 \quad \text{on } \partial\Omega_N \tag{2.14}$$

We note that the mobilities μ_n and μ_p generally depend on the electric field strength, i.e, on $|\nabla V|$ in a realistic model. Such a dependence could be incorporated in our subsequent analysis. However, since the technical details one has to deal with in this general case do not contribute to the understanding of inverse doping problems and their solution, we will assume that μ_n and μ_p are positive constants in the following, but we note that analogous mathematical results can be obtained if the mobilities are smooth functions of x, uniformly bounded away from 0 in Ω.

2.1 Existence and Regularity of Solutions

We first recall a fundamental result of existence of weak solutions; for the doping profile we will assume

$$C \in \mathcal{D} := \{\ C \in L^2(\Omega) \mid \underline{C} \le C \le \overline{C} \text{ a.e. in } \Omega\ \} \tag{2.15}$$

for some constants $\underline{C}, \overline{C} \in \mathbf{R}$.

Proposition 2.1. [40, Theorem 3.3.16] *Let $K \geq 1$ be chosen such that*

$$\frac{1}{K} \leq u_D(x), v_D(x) \leq K, \qquad \forall\, x \in \partial\Omega_D. \tag{2.16}$$

For any $C \in \mathcal{D}$, the boundary value problem (2.4)-(2.14) *admits a weak solution*

$$(V, u, v, J_n, J_p) \in H^1(\Omega)^3 \times L^2(\Omega)^2 \times L^2(\Omega)^2,$$

which satisfies

$$\min\left\{\tfrac{1}{K}, \ln\left(\tfrac{1}{2K\delta^2}(\underline{C} + \sqrt{\underline{C}^2 + 4\delta^4})\right)\right\} \leq V(x) \tag{2.17}$$

$$\leq \max\left\{K, U_T \ln\left(\tfrac{K}{2\delta^2}(\overline{C} + \sqrt{\overline{C}^2 + 4\delta^4}\right)\right\} \tag{2.18}$$

$$\tfrac{1}{K} \leq u(x) \leq K \tag{2.19}$$

$$\tfrac{1}{K} \leq v(x) \leq K \tag{2.20}$$

for almost all $x \in \Omega$.

For additional regularity of solutions we need the following assumption on the domain Ω and the parts Ω_D and Ω_N of its boundary, which we will use in the remainder of the paper:

Assumption 2.2. The solution w of

$$\Delta w = f \qquad \text{in } \Omega \tag{2.21}$$

$$w = g \qquad \text{on } \partial\Omega_D \tag{2.22}$$

$$\frac{\partial w}{\partial \nu} = 0 \qquad \text{on } \partial\Omega_N \tag{2.23}$$

satisfies

$$\|w\|_{W^{2,p}(\Omega)} \leq \gamma\left(\|f\|_{L^p(\Omega)} + \|g\|_{W^{2-\frac{1}{p},p}(\partial\Omega_D)}\right) \quad \text{for all } f \in L^p(\Omega), g \in W^{2-\frac{1}{p},p}(\partial\Omega_D) \tag{2.24}$$

for $p = \frac{3}{2}$ and $p = 2$.

The regularity class obtained for the solution is H^2 for the electric potential as well as for the equivalents of the electron and hole densities in Slootboom variables. We note that this also implies $(n, p) = (e^V u, e^{-V} v) \in H^2(\Omega)^2$:

Theorem 2.3. [38, Theorem 3.3.1] *Under the above assumptions every weak solution (V, u, v) of* (2.4)-(2.14) *satisfies*

$$(V, u, v) \in H^2(\Omega)^3.$$

The uniqueness of a solution can be shown only for small applied voltages, i.e., if U is sufficiently small in the norm of $L^\infty(\partial\Omega_D) \cap H^{\frac{3}{2}}(\partial\Omega_D)$.

Theorem 2.4. *Let $\|U\|_{L^\infty(\partial\Omega)} + \|U\|_{H^{\frac{3}{2}}(\partial\Omega_D)}$ be sufficiently small, then the solution (V, u, v) of* (2.4)-(2.14) *is unique in $H^1(\Omega)^3$.*

2.2 The Linearized Problem

In the following we shall analyze a linearized version of the system (2.4)-(2.14) in a quite general form, which allows to apply the results of this section to linearizations with respect to several parameters. The boundary value problem under investigation here is the formal linearization of the drift-diffusion equations at the state (V, u, v) with respect to variations in the doping profile and in the boundary data:

$$\lambda^2 \Delta \hat{V} = (e^V u + e^{-V} v)\hat{V} + e^V \hat{u} - e^{-V} \hat{v} + f_1 \qquad \text{in } \Omega \tag{2.25}$$

$$\begin{aligned} \text{div } (\mu_n e^V \nabla \hat{u}) &= -\text{div } (\mu_n e^V \hat{V} \nabla u) + Q(u,v,V,x)(u\hat{v} + \hat{u}v) \\ &\quad + Q'(u,v,V,x).(\hat{u},\hat{v},\hat{V})(uv-1) + f_2 \qquad \text{in } \Omega \end{aligned} \tag{2.26}$$

$$\begin{aligned} \text{div } (\mu_p e^{-V} \nabla \hat{v}) &= \text{div } (\mu_p e^{-V} \hat{V} \nabla v) + Q(u,v,V,x)(u\hat{v} + \hat{u}v) \\ &\quad + Q'(u,v,V,x).(\hat{u},\hat{v},\hat{V})(uv-1) + f_3 \qquad \text{in } \Omega \end{aligned} \tag{2.27}$$

$$\hat{V} = g_1 \qquad \text{on } \partial\Omega_D \tag{2.28}$$

$$\hat{u} = g_2 \qquad \text{on } \partial\Omega_D \tag{2.29}$$

$$\hat{v} = g_3 \qquad \text{on } \partial\Omega_D \tag{2.30}$$

$$\frac{\partial \hat{V}}{\partial \nu} = 0 \qquad \text{on } \partial\Omega_N \tag{2.31}$$

$$\frac{\partial \hat{u}}{\partial \nu} = 0 \qquad \text{on } \partial\Omega_N \tag{2.32}$$

$$\frac{\partial \hat{v}}{\partial \nu} = 0 \qquad \text{on } \partial\Omega_N, \tag{2.33}$$

with given functions

$$g_i \in H^{\frac{3}{2}}(\partial\Omega_D), \qquad f_i \in L^2(\Omega), i = 1, \ldots, 3$$

and $(V, u, v) \in H^2(\Omega)^3$, and unknowns $(\hat{V}, \hat{u}, \hat{v})$. By $Q'(u, v, V, x)$ we denote the vector $(\frac{\partial Q}{\partial u}, \frac{\partial Q}{\partial v}, \frac{\partial Q}{\partial V})$. We shall show that this system has a unique solution $(\hat{V}, \hat{u}, \hat{v})$ if the applied voltage U is sufficiently small, where the bound on U is independent of f_i and g_i. In the following we will always assume that the recombination-generation term Q is sufficiently smooth and satisfies

$$Q(u, v, V, x) \geq 0, \quad \forall\ (u, v, V, x) \in \mathbf{R}^+ \times \mathbf{R}^+ \times \mathbf{R} \times \Omega \tag{2.34}$$

which holds for all standard recombination-generation models (cf. [40]).

We start with some preliminary results concerning the single equations (2.25), (2.26) (2.27), respectively:

Lemma 2.5. *For given $\hat{u}$ and $\hat{v}$, the boundary value problem* (2.25), (2.28), (2.31) *has a unique solution $\hat{V} \in H^2(\Omega)$ and there exist continuous linear operators*

$$\begin{aligned} P &: H^1(\Omega)^2 \to H^2(\Omega) \\ S_1 &: L^2(\Omega) \to H^2(\Omega) \\ T_1 &: H^{\frac{3}{2}}(\partial\Omega_D) \to H^2(\Omega), \end{aligned}$$

such that

$$\hat{V} = P(\hat{u}, \hat{v}) + S_1 f_1 + T_1 g_1. \tag{2.35}$$

Moreover, there exists a constant $c_1 > 0$ (dependent on Ω, $\partial\Omega_D$ and λ only) such that the operator norm of P is bounded by

$$\|P\| \quad \leq \quad c_1 e^{\|V\|_{L^\infty(\Omega)}}. \tag{2.36}$$

Proof. The assertion follows from the standard theory of linear elliptic equations (cf. [26]). □

Now we turn our attention to the linearized continuity equations (2.26) and (2.27), which will be analyzed in the following lemma:

Lemma 2.6. *For given $\hat{V} \in H^2(\Omega)$, the coupled boundary value problem (2.26), (2.27), (2.29), (2.30),(2.32), (2.33) has a unique solution $(\hat{u}, \hat{v}) \in H^1(\Omega)^2$ and there exist continuous linear operators*

$$\begin{aligned} R \quad &: \quad H^1(\Omega) \to H^1(\Omega)^2 \\ S_2 \quad &: \quad L^2(\Omega)^2 \to H^1(\Omega)^2 \\ T_2 \quad &: \quad H^{\frac{1}{2}}(\partial\Omega_D)^2 \to H^1(\Omega)^2, \end{aligned}$$

such that

$$(\hat{u}, \hat{v}) = R\hat{V} + S_2(f_2, f_3) + T_2(g_2, g_3). \tag{2.37}$$

Proof. We rewrite the coupled boundary-value problem in its weak formulation, which consists of finding a pair $(\hat{u}, \hat{v}) \in H^1(\Omega)^2$, with boundary values given by (2.29) and (2.30), which satisfies

$$A(\hat{u}, \hat{v}; \phi, \psi) = \langle f, (\phi, \psi)\rangle, \qquad \forall\ (\phi, \psi) \in V_0, \tag{2.38}$$

where V_0 is the subspace of elements in $H^1(\Omega)^2$ with vanishing boundary values on $\partial\Omega_D$. The bilinear form A and the right-hand side f are defined by

$$\begin{aligned} A(\hat{u}, \hat{v}; \phi, \psi) \quad &= \quad \langle \mu_n e^V \nabla\hat{u}, \nabla\phi\rangle + \langle \mu_p e^{-V} \nabla\hat{v}, \nabla\psi\rangle + \langle Q(u\hat{v} + \hat{u}v), \phi + \psi\rangle \\ &\qquad + \langle Q_u \hat{u} + Q_v \hat{v}(uv - 1), \phi + \psi\rangle \\ \langle f, (\phi, \psi)\rangle \quad &= \quad \langle f_2, \phi\rangle + \langle f_3, \psi\rangle - \langle Q_V \hat{V}(uv - 1), \phi + \psi\rangle, \end{aligned}$$

where $\langle .,. \rangle$ denotes the scalar product on $L^2(\Omega)$. Since we have $f \in H^{-1}(\Omega)^2$, it suffices to show that A is a continuous and coercive bilinear form on $H_0^1(\Omega)$ by the Lax-Milgram lemma. The continuity can be shown by standard estimates and in order to verify the coercivity we estimate

$$\begin{aligned} A(\phi, \psi; \phi, \psi) \quad &= \quad \mu_p\langle e^V \nabla\phi, \nabla\phi\rangle + \mu_n\langle e^{-V} \nabla\psi, \nabla\psi\rangle + \langle Q(\phi + \psi), (\phi + \psi)\rangle \\ &\qquad + \langle Q((v - 1)\phi + (u - 1)\psi), \phi + \psi\rangle + \langle (Q_u\phi + Q_v\psi)(uv - 1), \phi + \psi\rangle \\ &\geq \quad \min\{\mu_n, \mu_p\} e^{-\|V\|_{L^\infty(\Omega)}} (\|\nabla\phi\|^2 + \|\nabla\psi\|^2) \\ &\qquad - |\langle Q((v - 1)\phi + (u - 1)\psi), \phi + \psi\rangle + \langle (Q_u\phi + Q_v\psi)(uv - 1), \phi + \psi\rangle|\,, \end{aligned}$$

where we have used the nonnegativity of Q. Since $u \to 1$ and $v \to 1$ in $L^\infty(\Omega)$ as $U \to 0$ (cf. [40]), for any $\epsilon > 0$ the estimate

$$|\langle Q((v - 1)\phi + (u - 1)\psi), \phi + \psi\rangle + \langle (Q_u\phi + Q_v\psi)(uv - 1), \phi + \psi\rangle| \leq \epsilon(\|\phi\|^2 + \|\psi\|^2)$$

holds for U sufficiently small. With the Poincaré inequality we obtain

$$A(\phi, \psi; \phi, \psi) \geq \left(\min\{\mu_n, \mu_p\} e^{-\|V\|_{L^\infty(\Omega)}} - \epsilon\right) (\|\nabla\phi\|^2 + \|\nabla\psi\|^2)$$

and another application of the Poincaré inequality yields coercivity for U sufficiently small. □

Using the preliminary results about the decoupled equations of the linearized system, we are now able to prove a regularity and stability result for the complete linear initial-value problem (2.25)-(2.33).

Theorem 2.7. *Let U be sufficiently small, then there exists a unique solution*

$$(\hat{V}, \hat{u}, \hat{v}) \in H^2(\Omega)^3$$

of the coupled boundary value problem (2.25)-(2.33), *which depends continuously on the functions f_i, g_i, $i = 1, 2, 3$ in the corresponding norms.*

Proof. Using the Lemmas 2.5 and 2.6 we may transform the system (2.25)-(2.33) into a linear problem of the form

$$\hat{V} - K\hat{V} = K_0(f_1, f_2, f_3, g_1, g_2, g_3)$$

with the continuous linear operators

$$K : H^2(\Omega) \to H^2(\Omega), \qquad K_0 : L^2(\Omega)^3 \times H^{\frac{1}{2}}(\partial\Omega_D)^2 \times H^{\frac{3}{2}}(\partial\Omega_D) \to H^2(\Omega)$$

defined by

$$K := PR$$
$$K_0(f_1, f_2, f_3, g_1, g_2, g_3) := S_1 f_1 + T_1 g_1 + P(S_2(f_2, f_3), T_2(g_2, g_3)).$$

A straight-forward estimate shows that $\|K\| < 1$ for U sufficiently small and hence, the Banach fixed-point theorem implies the existence and uniqueness of a solution $\hat{V} \in H^1(\Omega)$. Standard elliptic regularity theory (cf. [26]) finally implies the existence and uniqueness of a solution $(\hat{V}, \hat{u}, \hat{v}) \in H^2(\Omega)^3$ of the system (2.25)-(2.33). □

2.3 The Equilibrium Case

In the equilibrium case $U = 0$ further simplifications are possible. Since u and v are identically one on $\partial\Omega_D$ in this case, the unique solution (V, u, v) of (2.4)-(2.14) is given by $u = v = 1$ and by the solution V^0 of the equilibrium Poisson problem

$$\lambda^2 \Delta V^0 = e^{V^0} - e^{-V^0} - C \qquad \text{in } \Omega \tag{2.39}$$

$$V^0 = V_{bi} \qquad \text{on } \partial\Omega_D \tag{2.40}$$

$$\frac{\partial V^0}{\partial \nu} = 0 \qquad \text{on } \partial\Omega_N. \tag{2.41}$$

The directional derivative of the solution of the model equations (2.4)-(2.14) with respect to U in direction h at the point $U = 0$ is formally given by the solution $(\hat{V}, \hat{u}, \hat{v})$ of

$$\lambda^2 \Delta \hat{V} = e^{V^0}\hat{u} - e^{-V^0}\hat{v} + (e^{V^0} + e^{-V^0})\hat{V} \qquad \text{in } \Omega \tag{2.42}$$

$$\operatorname{div}\left(\mu_n e^{V^0} \nabla \hat{u}\right) = Q_0(V^0, x)(\hat{u} + \hat{v}) \qquad \text{in } \Omega \tag{2.43}$$

$$\operatorname{div}\left(\mu_p e^{-V^0} \nabla \hat{v}\right) = Q_0(V^0, x)(\hat{u} + \hat{v}) \qquad \text{in } \Omega, \tag{2.44}$$

where $Q_0(V^0,x) := Q(1,1,V^0)$. The linearized system is supplemented by the Dirichlet conditions

$$\hat{V} = h \qquad \text{on } \partial\Omega_D \tag{2.45}$$
$$\hat{u} = -h \qquad \text{on } \partial\Omega_D \tag{2.46}$$
$$\hat{v} = h \qquad \text{on } \partial\Omega_D \tag{2.47}$$

and the Neumann conditions

$$\frac{\partial \hat{V}}{\partial \nu} = 0 \qquad \text{on } \partial\Omega_N \tag{2.48}$$
$$\frac{\partial \hat{u}}{\partial \nu} = 0 \qquad \text{on } \partial\Omega_N \tag{2.49}$$
$$\frac{\partial \hat{v}}{\partial \nu} = 0 \qquad \text{on } \partial\Omega_N. \tag{2.50}$$

We note that $\hat{u}$ and $\hat{v}$ (as well as $\hat{J}_n$ and $\hat{J}_p$) do not depend on $\hat{V}$ and hence, if we are interested in outputs involving $\hat{u}$ and $\hat{v}$ only, the equation for $\hat{V}$ is superfluous.

3 Identification of Doping Profiles

In this section we introduce certain inverse problems for semiconductor devices and investigate their basic properties. For the moment we restrict our attention to the case close to equilibrium, for which we are able to give a mathematically rigouros treatment because of known uniqueness results and the existence of derivatives.

Our aim is to reconstruct a doping profile $C \in \mathcal{D}$ from indirect measurements. Possible measurements in practice are the current flow through a contact Γ_1 (cf. e.g. [38, 44]), which is given by

$$I(\Gamma_1) = \int_{\Gamma_1} (J_n + J_p).d\nu \tag{3.1}$$

and the mean capacitance of a contact (cf. e.g. [33]), i.e.,

$$Cap(\Gamma_1) = \frac{d}{dU}\left(\int_{\Gamma_1} \nabla V.d\nu\right). \tag{3.2}$$

For the identification of doping profiles, the amount of data obtained around equilibrium seems to be not sufficient in this case, since for each applied voltage one actually measures a single real number per contact and the outputs for different (small) applied voltages are strongly correlated. Consequently, one can only hope to identify a small number of parameters in an a-priorly specified model for the doping profile (an approach carried out by Khalil cf. [33]), but not a functional dependence. A possible way to overcome this problem is to consider 'global data', i.e., also measurements far away from equilibrium. However, besides existence proofs, the analysis of the drift-diffusion model for large applied voltages is not very well developed and therefore we shall not treat this case here, although we want to point out that this is an important and challenging problem for future research. Another possibility is to obtain more information by different ways of measuring data; in particular we consider pointwise measurements of the current density and the capacitance on a contact. Under industrial conditions this seems to be impossible so far, but in a laboratory a pointwise detection can be realized.

With this motivation we consider two possibilities of idealized data, which are given as follows:

Voltage-Current Data:

Voltage-Current data are given by measurements of the normal component of the current density $J.\nu = (J_n + J_p).\nu$ *on* $\Gamma_1 \subset \partial\Omega_D$ *for all applied voltages* $U \in H^{\frac{3}{2}}(\partial\Omega_D)$ *with* $\|U\| < r$ *with some small* $r > 0$. *We assume that* $J.\nu|_{\Gamma_1} \in L^2(\Gamma_1)$ holds.

Capacitance Data:

Capacitance data are measurements of the variation of the electric flux in normal outward direction ($\frac{\partial V}{\partial \nu}$ *on* $\Gamma_1 \subset \partial\Omega_D$) *with respect to the voltage* Φ, *i.e.,* $\lim_{s\to 0} s^{-1}(\frac{\partial V^{s\Phi}}{\partial \nu} - \frac{\partial V^0}{\partial \nu})|_{\Gamma_1} \in L^2(\Gamma_1)$, *for all voltages* $\Phi \in H^{\frac{3}{2}}(\partial\Omega_D)$, *where* V^Φ *denotes the solution of the Poisson equation with* $U = \Phi$.

We note that the capacitance data defined above are just the ones at equilibrium. Alternatively, one could consider variations around any other applied voltage U and the analysis could be carried out in an analogous way, provided U is sufficiently small. However, since we perform only a preliminary study of the capacitance data here, we restrict ourselves to the equilibrium case.

In both cases we assume that Γ_1 is a sufficiently regular subset of $\partial\Omega_D$ with nonzero measure. Unless further noted we shall consider the case of current measurements, but in a separate analysis we will also treat capacitance measurements. The basic property, which we need, is that for each voltage U (with norm bounded by r sufficiently small) as input of the system, the corresponding output, namely the normal current density $J.\nu$ is well-defined. In other words, we have to show that the map $U \mapsto J.\nu$ is well-defined in appropriate spaces, which will be the objective of the following subsection.

3.1 The Voltage-Current Map

In this section we will investigate the *voltage-current map*, i.e., the relation between the applied voltage U and the normal component of the current density on a part of the boundary. For the moment we fix the doping profile C, but since our final goal is to investigate the dependence of the voltage-current relation on the specific choice of C and to invert this relation, we introduce a subscript for the doping profile in our notation. We define the voltage-current map Σ_C via

$$\begin{array}{rrcl} \Sigma_C: & B_r(0) \subset H^{\frac{3}{2}}(\partial\Omega_D) & \to & L^2(\Gamma_1) \\ & U & \mapsto & J.\nu|_{\Gamma_1}, \end{array} \tag{3.3}$$

We first verify that the nonlinear operator Σ_C is well-defined and investigate its smoothness properties:

Proposition 3.1. *For each applied voltage* $U \in B_r(0) \subset H^{\frac{3}{2}}(\partial\Omega_D)$, *the current* $J.\nu = (J_n + J_p).\nu \in L^2(\Gamma_1)$ *is uniquely defined. Furthermore, the map* Σ_C *is continuous between these spaces, continuously Frèchet-differentiable on* $B_r(0)$ *and*

$$\Sigma_C'(U)\Phi = \mu_n e^{V_D} \frac{\partial \hat{u}}{\partial \nu} - \mu_p e^{-V_D} \frac{\partial \hat{v}}{\partial \nu} + \left(\mu_n e^{V_D} \frac{\partial u}{\partial \nu} + \mu_p e^{-V_D} \frac{\partial v}{\partial \nu}\right) \hat{V}, \tag{3.4}$$

where $(\hat{V}, \hat{u}, \hat{v})$ *solves* (2.25)-(2.33) *with*

$$\begin{array}{lll} f_1 = 0 & f_2 = 0 & f_3 = 0 \\ g_1 = \Phi & g_2 = -e^{-V_D} n_D \Phi & g_3 = e^{V_D} p_D \Phi. \end{array} \tag{3.5}$$

Proof. The nonlinear system (2.4)-(2.14) has a unique solution $(V, u, v) \in H^2(\Omega)^3$ and therefore ∇u and ∇v have a trace in $H^{\frac{1}{2}} \subset L^2(\Gamma_1)$. Since V^0 is continuous on $\overline{\Omega}$, we obtain

$$J.\nu = \mu_n e^{V_D} \frac{\partial u}{\partial \nu} - \mu_p e^{-V_D} \frac{\partial v}{\partial \nu} \in L^2(\Gamma_1)$$

is well-defined and depends continuously on U. The Frèchet-differentiability follows from a straight-forward estimate of the residual $\Sigma_C(U + \Phi) - \Sigma_C(U) - \Sigma_C'(U)\Phi$ together with Theorem 2.7. □

By iterating the above procedure we can show further regularity of the nonlinear operator Σ_C:

Proposition 3.2. *The voltage current map* Σ_C *is an element of* $C^\infty(B_r(0); L^2(\Gamma_1))$.

Sketch of Proof. The n-th derivative is of the form (2.25)-(2.33) with right-hand sides f_j and boundary values g_j that depend in a Lipschitz-continuous way on the solution (V, u, v) of the direct problem and the first $n-1$ derivatives. Similar arguments to the proof of Proposition 3.1 show that this derivative is a Frèchet-derivative of n-th order and continuous. □

3.2 Identification of Doping Profiles from Full Voltage-Current Data

In the following we treat the identification of doping profiles in a rather general setup. A realistic set of data is to measure for given U_j with $\|U_j\| = 1$ the outputs

$$\{ \ \Sigma_C(tU_j) \mid j = 1, \ldots, N, t \in [0, r) \ \}.$$

In practical applications, the functions U_j are piecewise constant on the contacts. The amplitude t of an applied voltage can be varied almost continuously in an experiment, which is the motivation for our specific choice of the data set.

The continuity of Σ_C implies in particular that the map $t \mapsto \Sigma_C(tU_j)$ is continuous for fixed U_j and therefore

$$\Sigma_C(.U_j) \in C(0, r; L^2(\Gamma_1)) \hookrightarrow L^2(0, r; L^2(\Gamma_1)) = L^2((0, r) \times \Gamma_1).$$

Since it seems more realistic to bound the measurement error in an L^2-norm than in a stronger norm we consider the data as

$$Y := (\Sigma_C(.U_j))_{j=1,\ldots,N} \in L^2((0, r) \times \Gamma_1)^N. \tag{3.6}$$

To apply the standard theory for inverse problems, we write the identification problem in the abstract form

$$F(C) = Y, \tag{3.7}$$

where Y are the given data and C is the parameter to be identified, in our case the doping profile. In order to transform our identification problem into the form (3.7), we have to define the *parameter-to-output map* F, which maps the input of the system (the parameter C) to the output Y, on appropriate function spaces. As the domain of the operator we choose

$$\mathcal{D} := \{ \, C \in L^2(\Omega) \mid \underline{C} \leq C \leq \overline{C} \text{ a.e. in } \Omega \, \} \tag{3.8}$$

for appropriate upper and lower bounds $\underline{C}$ and $\overline{C}$. This choice of the domain is motivated by the existence results for the drift-diffusion equations, which show that for $t \, \|U_j\| < r$ (r sufficiently small) and $C \in \mathcal{D}$ a unique solution exists and therefore, the map

$$\begin{array}{rcl} F: \; \mathcal{D} & \to & L^2((0,r) \times \Gamma_1)^N \\ C & \mapsto & (\Sigma_C(.U_j))_{j=1,\ldots,N} \end{array} \tag{3.9}$$

is well-defined.

Proposition 3.3. *The parameter-to-output map F is well-defined by* (3.9) *and Frèchet-differentiable on $\mathcal{D}$.*

Proof. The well-definedness follows immediately from Proposition 3.1, which shows that for each doping profile $C \in \mathcal{D}$, the voltage-current map is well-defined and therefore there exists a unique output vector Y.

In order to show Frèchet-differentiability of F it suffices to show the differentiability of the map $C \mapsto (V,u,v) \in H^2(\Omega)^3$ for fixed U_j, since the differentiability of the map $(V,u,v) \mapsto J.\nu|_{\Gamma_1}$ has already been shown in the analysis of the voltage-current map. The derivative $(\hat{V}, \hat{u}, \hat{v})$ of the drift-diffusion equations with respect to a variation $\hat{C}$ of the doping profile is given by the solution of (2.25)-(2.33) with $g_i = 0$, $f_1 = -\hat{C}$ and $f_2 = f_3 = 0$. Hence, the derivative with respect to the doping profile exists and depends continuously on $\hat{C}$ by Theorem 2.7. An estimate of the remainder, which shows that the derivative is Frèchet, can be carried out in a similar way as in the proof of Proposition 3.1. □

3.3 Identification from Reduced Voltage-Current Data

Since the voltage-current map can in general be defined only in a neighborhood of $U = 0$ due to possible hysteresis effects for large applied voltage (cf. e.g. [40]), it seems reasonable to consider the problem of identifying the doping profile from the linearization of the voltage-current map at $U = 0$. The advantage of this is that the Poisson equation and the continuity equations decouple as we shall see below and therefore the complexity of the problem reduces significantly.

The derivative in direction Φ is given as

$$\mathcal{S}_C \Phi := \Sigma'_C(0)\Phi = \left(\mu_n e^{V_{bi}} \frac{\partial \hat{u}}{\partial \nu} - \mu_p e^{-V_{bi}} \frac{\partial \hat{v}}{\partial \nu} \right) |_{\partial\Omega_D}, \tag{3.10}$$

where $(\hat{u}, \hat{v})$ is the solution of the boundary-value problem

$$\operatorname{div}\left(\mu_n e^{V^0} \nabla \hat{u}\right) = Q_0(V^0,x)(\hat{u}+\hat{v}) \quad \operatorname{div}\left(\mu_p e^{-V^0} \nabla \hat{v}\right) = Q_0(V^0,x)(\hat{u}+\hat{v}) \quad \text{in } \Omega \tag{3.11}$$

$$\hat{u} = -\Phi \qquad\qquad \hat{v} = \Phi \qquad\qquad \text{on } \partial\Omega_D \tag{3.12}$$

$$\frac{\partial \hat{u}}{\partial \nu} = 0 \qquad\qquad \frac{\partial \hat{v}}{\partial \nu} = 0 \qquad\qquad \text{on } \partial\Omega_N. \tag{3.13}$$

and V^0 is the solution of the equilibrium problem (2.39)-(2.41).

The linear operator $\mathcal{S}_C$ maps $H^{\frac{3}{2}}(\partial\Omega_D)$ to $L^2(\Gamma_1)$, it is continuous and compact as we will show in the following Lemma:

Lemma 3.4. *The linear operator $\mathcal{S}_C$ is bounded and compact.*

Proof. Standard variational and regularity arguments imply that $(\hat{u}, \hat{v}) \in H^2(\Omega)^2$ depends continuously on the input $\|\Phi\|_{H^{\frac{3}{2}}(\partial\Omega_D)}$ and hence, the boundedness and compactness of $\mathcal{S}_C$ follow directly from the compactness of the trace maps

$$\hat{u} \mapsto \frac{\partial \hat{u}}{\partial \nu}|_{\partial\Omega_D} \qquad \text{and } \hat{v} \mapsto \frac{\partial \hat{v}}{\partial \nu}|_{\partial\Omega_D}$$

from $H^2(\Omega)$ to $L^2(\partial\Omega_D)$. □

We note that in the process of computing $\Sigma_C'(0)$ from the given data Σ_C in $B_\rho(0)$, data have to be differentiated, which is an ill-posed step in principle, but since we know that Σ_C is smooth and we can give bounds on the derivatives (see Proposition 3.2), this part of the problem becomes well-posed (by compactness).

Contrary to the case of full data, the solution $V = V(C)$ of the Poisson equation can be computed a-priori now, since it is independent of Φ. The remaining problem (3.11)-(3.13) is quite similar to the problem in *electrical impedance tomography* (also called *inverse conductivity problem*, cf. e.g. [15, 34] and the references quoted there), where the aim is to identify the conductivity $a = a(x)$ in the equation

$$-\text{div } (a\nabla u) = f \tag{3.14}$$

from a measurement of the *Dirichlet-to-Neumann map*, which maps the applied voltage $u|_{\partial\Omega}$ to the electrical flux $a\frac{\partial u}{\partial \nu}|_{\partial\Omega}$, where u is the electric potential. The linearized voltage-current map $\mathcal{S}_C$, which appears in our application maps the Dirichlet data for u and v to the sum of their Neumann data. Hence, this identification problem for doping profiles in semiconductor devices can be seen as the counterpart of electrical impedance tomography for common conducting materials.

If we assume that the full data are given by (3.6), we can compute reduced data as

$$Z := (\mathcal{S}_C U_j)_{j=1,\dots,N} \in L^2(\Gamma_1)^N. \tag{3.15}$$

This allows to define the parameter-to-output map for reduced data as

$$\begin{array}{llll} G: & \mathcal{D} \subset L^2(\Omega) & \to & L^2(\Gamma_1)^N \\ & C & \mapsto & (\mathcal{S}_C U_j)_{j=1,\dots,N} . \end{array} \tag{3.16}$$

The well-definedness and differentiability of the nonlinear operator G can be shown in an analogous way to Proposition 3.3

3.4 Identification of Doping Profiles from Capacitance Measurements

In this section we consider the inverse doping problem for semiconductor devices with capacitance measurements. Similar to the case of reduced voltage-current data, we can compute the capacitance as

$$\mathcal{T}_C \Phi = \frac{\partial \hat{V}}{\partial \nu}|_{\Gamma_1}, \tag{3.17}$$

where $\hat{V}$ solves

$$\lambda^2 \Delta \hat{V} = \left(e^{V^0} + e^{-V^0}\right) \hat{V} + e^{V^0} \hat{u} - e^{-V^0} \hat{v}. \tag{3.18}$$

V^0 is the potential in the equilibrium problem (2.39)-(2.41) and $(\hat{u}, \hat{v})$ is the solution of (3.11)-(3.13). In addition, $\hat{V}$ satisfies the boundary conditions

$$\hat{V} = \Phi \qquad \text{on } \partial\Omega_D \tag{3.19}$$

$$\frac{\partial \hat{V}}{\partial \nu} = 0 \qquad \text{on } \partial\Omega_N. \tag{3.20}$$

Since we have seen in the previous sections that the map $\Phi \mapsto (\hat{u}, \hat{v}) \in H^2(\Omega)^2$ is well-defined an continuous, we obtain the well-definedness and continuity of the capacitance map $\mathcal{T}_C$ as a direct consequence, since the solution $\hat{V}$ depends continuously on the boundary data and on $\hat{u}$ and $\hat{v}$, which appear in the right-hand side. Similar to Lemma 3.4 we can show the following preliminary result:

Lemma 3.5. *The linear operator $\mathcal{T}_C : H^{\frac{3}{2}}(\partial\Omega_D) \to L^2(\Gamma_1)$ is bounded and compact.*

More realistic data in this case are measurements of

$$\tilde{Z} := (\mathcal{T}_C U_j)_{j=1,\ldots,N} \in L^2(\Gamma_1)^N, \tag{3.21}$$

for given U_j with $\|U_j\| = 1$, and the corresponding parameter-to-output map is defined by

$$\begin{array}{llcl} H: & \mathcal{D} \subset L^2(\Omega) & \to & L^2(\Gamma_1)^N \\ & C & \mapsto & (\mathcal{T}_C U_j)_{j=1,\ldots,N}. \end{array} \tag{3.22}$$

The parameter-to-output map H in this case is well-defined and Frèchet-differentiable, which follows immediately from the well-definedness of the trace-type map $V \mapsto \frac{\partial V}{\partial \nu}|_{\Gamma_1}$ and the proof of Proposition 3.3, where the differentiability of the map $C \mapsto V \in H^2(\Omega)$ has been verified.

3.5 The Limit of Zero Space Charge

An important limiting case of the drift-diffusion equations is the limit of *zero space charge*, which means in mathematical terms that $\lambda \to 0$. We now want to discuss some properties of the parameter-to-output maps in this limit. It has been shown that a solution $(V, u, v) \in L^\infty(\Omega)^3$ still exists (cf. [37, 40]) for the reduced problem, but there is no additional regularity statement on the potential V.

One observes that capacitance measurements might not be possible for $\lambda = 0$, since the normal derivative of the potential V may not be well-defined in this case, unless C is sufficiently smooth. However, this difficulty could be overcome by restricting the set of admissible doping profiles, such that a normal derivative of C exists on Γ_1, e.g. we could choose $C \in H^2(\Omega)$. In the above setup we may still consider the voltage-current map for $\lambda = 0$, since we still have a normal derivative of u and v. The main problem in this case is that without further regularity on C we can only guarantee $(u, v) \in H^1(\Omega)^2$ and therefore $J.\nu \in H^{-\frac{1}{2}}(\Gamma_1)$. However, if $\nabla C \in L^p(\Omega)$ with $p \geq 6$ one can show by similar reasoning to the proof of regularity results for the drift-diffusion equation that the reduced voltage-current map exists and maps continuous to $L^2(\Gamma_1)$.

The Poisson equation at equilibrium reduces in this case to the algebraic relation $\sinh V = 2C$ and therefore we can rewrite the linearized continuity equations in the form

$$\begin{aligned} \mathrm{div}\ (\mu_n a \nabla \hat{u}) &= q(a,x)(\hat{u}+\hat{v}) && (3.23)\\ \mathrm{div}\ (\mu_p a^{-1} \nabla \hat{v}) &= q(a,x)(\hat{u}+\hat{v}), && (3.24)\end{aligned}$$

with

$$a = a(C) = e^{\operatorname{arcsinh}(2C)}, \qquad q(a,x) = Q(1,1,\ln(a),x), \tag{3.25}$$

and hence, we can reformulate the inverse problem as the identification of the conductivity a in (3.23), (3.24) from the reduced voltage-current map. From the knowledge of a we can then easily reconstruct $C = \frac{1}{2}\sinh(\ln a)$.

4 Identifiability: The Unipolar Case

In this section we want to investigate the problem of identifiability, i.e., we treat the question whether the data determine the doping uniquely. In the most general setup we cannot give an answer to this problem, but we are able to show the identifiability of the doping profile from reduced voltage-current data in the unipolar case, i.e., if $p = 0$ or, equivalently, $v = 1$. In addition, we assume that there is no recombination-generation, i.e., $Q = 0$, which seems reasonable in this case close to equilibrium. Since the basic structure of the problem is not different in the bipolar case, this suggests the assertion that the doping profile is identifiable also in the bipolar case. Since all information on the reduced data set is also contained in the full data, this would imply identifiability in the general case, too.

For reduced voltage-current data given on the whole boundary $\partial\Omega$, the inverse problem consists of identifying the parameter C in the system

$$\begin{aligned} \lambda^2 \Delta V^0 &= e^{V^0} - e^{-V^0} - C && \text{in } \Omega && (4.1)\\ \mathrm{div}\ \left(e^{V^0}\nabla \hat{u}\right) &= 0 && \text{in } \Omega && (4.2)\\ V^0 &= V_{bi} && \text{on } \partial\Omega && (4.3)\end{aligned}$$

from the Dirichlet-to-Neumann map $\hat{u}|_{\partial\Omega} \mapsto \frac{\partial \hat{u}}{\partial \nu}|_{\partial\Omega}$. We note that since $V^0 = V_{bi}$ is known on $\partial\Omega$ we can replace the current data $J = \mu_n e^{V^0}\frac{\partial \hat{u}}{\partial \nu}$ directly by the Neumann data $\frac{\partial \hat{u}}{\partial \nu}$.

In order to investigate the question of identifiability, we split the problem into two parts: first, the potential V (respectively e^V) can be identified from the Dirichlet-to-Neumann map for the density u and as the second step we consider the identification of C from V in (4.1). We rewrite the first step as the identification of the conductivity γ in the elliptic equation

$$\mathrm{div}\ (\gamma \nabla u) = 0. \tag{4.4}$$

For this problem, a uniqueness result has been shown by Nachman in two dimensions:

Theorem 4.1. *[41, Theorem 1] let $\Omega \subset \mathbf{R}^2$ be a bounded Lipschitz domain and let $\gamma_i \in L^\infty(\Omega) \cap W^{2,p}(\Omega)$ $(i = 1,2)$ for some $p > 1$ with positive lower bound. Then the equality of the Dirichlet-to-Neumann maps*

$$\begin{array}{rccc} \Lambda_i : & H^{\frac{1}{2}}(\partial\Omega) & \to & H^{-\frac{1}{2}}(\partial\Omega) \\ & u & \mapsto & \frac{\partial u}{\partial \nu} \end{array} \tag{4.5}$$

for the solutions u of (4.4) implies $\gamma_1 = \gamma_2$.

This result can be used to prove the identifiability of the doping profile in the unipolar case:

Theorem 4.2. *Let $\Omega \subset \mathbf{R}^2$ be a bounded Lipschitz domain and let $\Gamma_1 = \partial\Omega_D = \partial\Omega$, then for two doping profiles C_1 and C_2 in $\mathcal{D}$, the equality $\mathcal{S}_{C_1} = \mathcal{S}_{C_2}$ implies $C_1 = C_2$.*

Proof. Proposition 2.1 and Theorem 2.3 imply that for each $C \in \mathcal{D}$ the corresponding solution V of (4.1) is bounded below and satisfies $V \in H^2(\Omega)$. Therefore the function $\gamma := e^V$ is strictly positive and satisfies $\gamma \in L^\infty(\Omega)$ because of $V^0 \in L^\infty(\Omega)$. Furthermore we have $\nabla\gamma = e^{V^0}\nabla V^0 \in L^2(\Omega)^2$ and

$$\nabla^2\gamma = e^{V^0}\left(\nabla^2 V^0 + \nabla V^0(\nabla V^0)^T\right) \in L^2(\Omega)^{2\times 2}$$

(note that due to the embedding $H^2(\Omega) \hookrightarrow W^{1,4}(\Omega)$ we have $\nabla V^0(\nabla V^0)^T \in L^2(\Omega)^{2\times 2}$), and hence, $\gamma \in H^2(\Omega)$. Consequently, all assumptions of Theorem 4.1 are satisfied and hence, the potential $V^0 \in H^2(\Omega)$ is uniquely determined by the reduced voltage-current map $\mathcal{S}_C$. Then, (4.1) gives the uniqueness of C. □

We note that due to a result by Brown and Uhlmann [9] the identifiability result for the inverse conductivity problem (Theorem 4.1) can be extended to conductivities in $W^{1,p}(\Omega)$, $p > 2$. This result is of particular interest for the case of zero space charge ($\lambda = 0$) in the unipolar drift-diffusion equations and allows to show the identifiability of doping profiles $C \in L^\infty(\Omega) \cap W^{1,p}(\Omega)$ also there.

We note that the identifiability results are strongly dimension-dependent. In the one-dimensional case the data obviously do not suffice, whereas the parameter is well-determined in two dimensions as we have seen above. The analysis of the inverse conductivity problem in dimension $d \geq 3$ (cf. [50]) shows that the identification problem is even overdetermined in higher dimensions.

Stability estimates for the inverse conductivity problem in two dimensions can hardly be found in literature, the few existing results such as the ones by Sun [49] use very restrictive assumptions on the conductivity, which contradict the situation for inverse doping problems. However, the results in the three-dimensional case (cf. e.g. [1]), where the problem is overdetermined, already show severe ill-posedness and therefore one can argue that the two-dimensional case is also severely ill-posed.

Identifiability in the case of capacitance measurements cannot be shown by analogy to well-investigated inverse problems, since it the system cannot be decoupled in this case. A similar problem arises also for voltage-current data in the bipolar case, where the continuity equations are still coupled. Since identifiability of parameters in systems of differential equations is a hardly investigated topic, we will leave this problem as a challenging task for future research.

5 Piecewise Constant Profiles: The P-N Diode

In the following we shall focus on the simplest-case of a semiconductor device, namely the p-n diode. This special device has two Ohmic contacts at Γ_1 and $\Gamma_0 = \partial\Omega_D - \Gamma_1$ (see Figure 1), with applied potential

$$U(x) = \begin{cases} U & \text{for } x \in \Gamma_1 \\ 0 & \text{for } x \in \partial\Omega_D - \Gamma_1 \end{cases} . \tag{5.1}$$

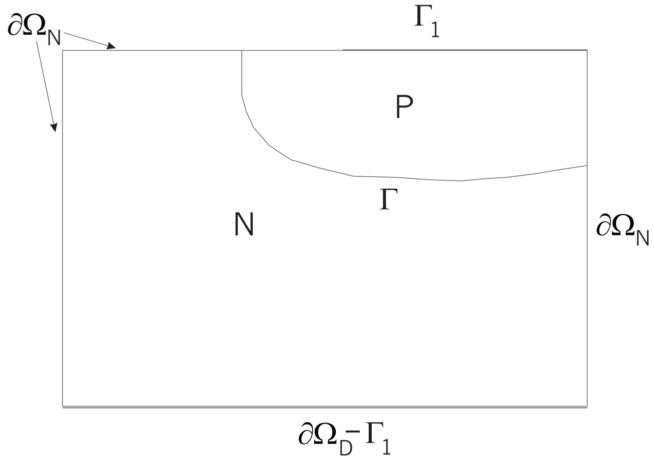

Figure 1: Two-dimensional cross section of a p-n diode.

The domain is split into two subregions P and N with $C > 0$ in P and $C > 0$ in N. The curve Γ between these regions is usually called *p-n junction.*

Furthermore we restrict our attention to piecewise constant doping profiles, i.e. the doping profile can be written as

$$C = c_1 \chi_P + c_2 \chi_N, \tag{5.2}$$

with real constants $c_1 > 0$ and $c_2 < 0$, where χ_P and χ_N denote the indicator functions of the domains P and N. Due to this restriction of the doping profile, the quantity to be identified is now the curve Γ that separates the regions P and N and possibly the two real numbers c_1 and c_2. Since this a-priori assumption on the doping profile reduces the complexity of the identification problem, it is possible to restrict the data, too. Instead of measuring the whole current-voltage map one can also consider the identification from a single measurement, which is often the case in practice, since the input voltage U is kept constant over each contact.

5.1 Restriction of the Data

We assume that we can measure the normal component of the current on a part of the boundary for each applied voltage in a small ball around $U = 0$, i.e., we know

$$I_C(U) := J^U.\nu|_{\Gamma_1}, \quad \forall\, |U| < r, \tag{5.3}$$

with $r > 0$, $\Gamma_1 \subset \partial\Omega_D$ and ν the outer normal on Γ_1. In (5.3), $J^U = J_n^U + J_p^U$, where $(V^U, u^U, v^U, J_n^U, J_p^U)$ is the solution of (2.4)-(2.14) with applied voltage (5.1). The subscript C indicates that I_C is the outflow current for a particular doping profile C.

For all $C \in L^\infty(\Omega)$, $I_C(U)$ is a function on Γ_1 for each $U \in (-r, r)$ and since for sufficiently small r, the solution of the direct problem is unique, the vector-valued function $I : U \mapsto J^U.\nu|_{\Gamma_1}$ is well-defined on the real interval $(-r, r)$; furthermore we have

$$I_C \in C^\infty(-r, r; L^2(\Gamma_1)). \tag{5.4}$$

Similar to the restriction of the voltage-current data to the linearization around equilibrium in Section 3.3, we can also use reduced data in this particular case. For this sake we have to determine the derivative of I_C at $U=0$ with respect to U, which exists since I_C is sufficiently smooth and is given by

$$g_C := \frac{dI_C}{dU}(0) = \left(\mu_n e^{V^0}\frac{\partial \hat{u}}{\partial \nu} - \mu_p e^{-V^0}\frac{\partial \hat{v}}{\partial \nu}\right)|_{\Gamma_1} \tag{5.5}$$

where $(\hat{u},\hat{v})$ is the solution of the boundary-value problem

$$\mathrm{div}\left(\mu_n e^{V^0}\nabla \hat{u}\right) = Q_0(V^0,x)(\hat{u}+\hat{v}) \qquad \mathrm{div}\left(\mu_p e^{-V^0}\nabla \hat{v}\right) = Q_0(V^0,x)(\hat{u}+\hat{v}) \quad \text{in } \Omega \tag{5.6}$$

$$\hat{u} = -1 \qquad \hat{v} = 1 \qquad \text{on } \Gamma_0 \tag{5.7}$$

$$\hat{u} = 0 \qquad \hat{v} = 0 \qquad \text{on } \partial\Omega_D - \Gamma_0 \tag{5.8}$$

$$\frac{\partial \hat{u}}{\partial \nu} = 0 \qquad \frac{\partial \hat{v}}{\partial \nu} = 0 \qquad \text{on } \partial\Omega_N. \tag{5.9}$$

and V^0 is the solution of the equilibrium problem (2.39)-(2.41). The linearization at the point $U=0$ is just a function on Γ_1, we will call g_C the *reduced output current.* As a direct consequence of (5.4) we obtain that $g_C(t) = \mathcal{S}_C(t\chi_{\Gamma_0}) \in L^2(\Gamma_1)$ for all $C \in \mathcal{D}$.

5.2 Setup of the Inverse Problem

For the reduced data, the inverse problem consists in identifying the doping profile C of the form (5.2) from the knowledge of g_C. For this sake we define the *parameter-to-output map*

$$\begin{array}{rccc} M: & \mathcal{D}(M) & \to & L^2(\Gamma_1) \\ & (c_1,c_2,\Gamma) & \mapsto & g_{c_1\chi_P + c_2\chi_N}. \end{array} \tag{5.10}$$

The parameter-to-output map assigns to each admissible parameter (C respectively (c_1,c_2,Γ)) the resulting output (g_C) that corresponds to the type of data. Hence, the inverse problem is just the (approximate) solution of the nonlinear operator equation

$$M(c_1,c_2,\Gamma) = g^\delta, \tag{5.11}$$

where g^δ represents a noisy observation of the reduced output current.

We note that M is the concatenation of the maps $(c_1,c_2,\Gamma) \mapsto c_1\chi_{P(\Gamma)} + c_2\chi_{N(\Gamma)}$ and $C \mapsto g_C$, where $N(\Gamma)$ and $P(\Gamma)$ are the two subregions separated by Γ.

5.3 Limiting Cases

In the following we consider limiting cases of parameters in the drift-diffusion equations (2.4)-(2.14), now in the case of a p-n diode, where further simplifications are possible. Of particular interest is now the case of zero space charge ($\lambda = 0$), for which the equation (2.39) simplifies to an algebraic relation between the potential V and the doping profile C. In this case we can compute $V = \operatorname{arcsinh}\frac{C}{2}$ explicitly and therefore we may rewrite the problem as the identification of a function V of the form $V = a + b\chi_N$ in (5.6)-(5.9), where

$$a = \operatorname{arcsinh}\frac{c_1}{2}, \qquad b = \operatorname{arcsinh}\frac{c_2}{2} - \operatorname{arcsinh}\frac{c_1}{2}.$$

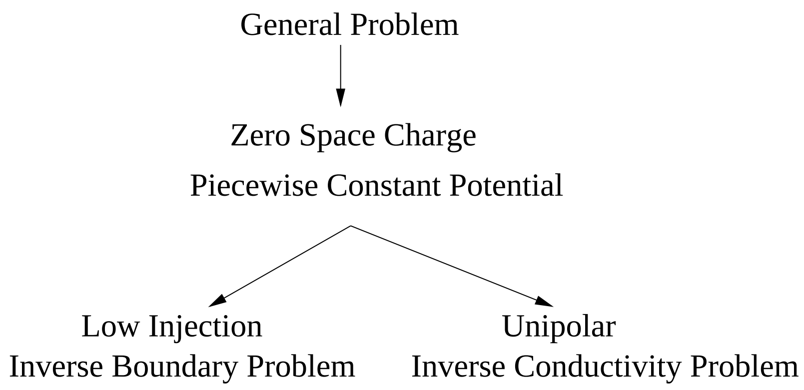

Figure 2: Limiting cases and corresponding inverse problems.

In the following we will investigate two subcases, first the one with low injection and later the unipolar case. It will turn out that the first leads to an inverse boundary problem, while the second can be reduced to the inverse conductivity problem with a single measurement.

5.3.1 Zero Space Charge and Low Injection

The case of zero space charge and low injection means to let first tend $\lambda \to 0$ and then $\delta \to 0$ in (2.4)-(2.6), which causes in particular the recombination-generation term to vanish. It has been shown by Schmeiser [43] that the arising limiting problem for u and v has a unique solution close to equilibrium, which is given by

$$u = \begin{cases} 1 + (e^U - 1)\hat{u} & \text{in } P \\ e^U & \text{in } N \end{cases} \tag{5.12}$$

$$v = \begin{cases} e^{-U} + (1 - e^{-U})\hat{v} & \text{in } N \\ 1 & \text{in } P \end{cases}, \tag{5.13}$$

where $(\hat{u}, \hat{v})$ solve

$$-\mathrm{div}\left(\frac{\mu_n}{|C|}\nabla\hat{u}\right) = 0 \qquad \text{in } P \tag{5.14}$$

$$\hat{u} = 1 \qquad \text{on } \Gamma \tag{5.15}$$

$$\hat{u} = 0 \qquad \text{on } \Gamma_1 \tag{5.16}$$

$$\frac{\partial \hat{u}}{\partial \nu} = 0 \qquad \text{on } \partial\Omega_N \cap \partial P \tag{5.17}$$

and

$$-\mathrm{div}\left(\frac{\mu_p}{C}\nabla\hat{v}\right) = 0 \qquad \text{in } N \tag{5.18}$$

$$\hat{v} = 1 \qquad \text{on } \Gamma \tag{5.19}$$

$$\hat{v} = 0 \qquad \text{on } \Gamma_0 \tag{5.20}$$

$$\frac{\partial \hat{v}}{\partial \nu} = 0 \qquad \text{on } \partial\Omega_N \cap \partial N. \tag{5.21}$$

For constant μ_n, μ_p and piecewise constant doping profile, the functions $\hat{u}$ and $\hat{v}$ just solve Laplace equations in P and N, respectively. The current is given by

$$J = (e^U - 1)\frac{\mu_n}{|C|}\nabla\hat{u} \tag{5.22}$$

and hence, in this limiting case the reduced data contain exactly the same information about the doping profile as the complete set of data.

Assuming that we know C on $\partial\Omega$, for the identification of the junction Γ it suffices to consider the function $w = \hat{u} - 1$. Then w solves the problem

$$-\Delta w = 0 \qquad \text{in } P \tag{5.23}$$

$$w = 0 \qquad \text{on } \Gamma \tag{5.24}$$

$$w = -1 \qquad \text{on } \Gamma_1 \tag{5.25}$$

$$\frac{\partial w}{\partial \nu} = d \qquad \text{on } \partial P - \Gamma \tag{5.26}$$

with $d = 0$ on $\partial\Omega_N \cap \partial P$ and $d = \frac{|C|}{\mu_n} g_C$ on Γ_1. In this case the problem of identifying the junction Γ can then be interpreted as an inverse boundary problem similar to the ones considered by Beretta et. al. [3, 6] for pure Neumann or pure Dirichlet conditions. In these cases it is known that the problem is exponentially ill-posed, i.e., an error of order ϵ in the boundary values leads to an error of order $|\ln\epsilon|^{-\nu}$ for some $\nu \in \mathbf{R}^+$ in the reconstruction of the domain P even under strong a-priori assumptions on Γ.

The identifiability result shown by Beretta et. al. [3] can be extended to the case of mixed boundary data in the following way:

Theorem 5.1 (Identifiability). *Let w and $\overline{w}$ be two solutions of (5.23)-(5.26) with corresponding junctions Γ and $\tilde{\Gamma}$ sufficiently smooth and such that $\Gamma_1 \subset P \cap \tilde{P}$. Then the equality of Dirichlet and Neumann values on Γ_1 implies $\Gamma = \tilde{\Gamma}$.*

Proof. Let $z = w - \overline{w}$, then z has homogeneous Neumann and Dirichlet values on Γ_1 and satisfies $\Delta z = 0$ in $P \cap \tilde{P}$. Hence, the uniqueness of the Cauchy problem for elliptic equations and analytic continuation for harmonic functions implies $z = 0$ in the closure of $P \cap \tilde{P}$. Since either $w = 0$ or $\overline{w} = 0$ on $\partial(P \cap \tilde{P}) - \partial\Omega$, we obtain $w = \overline{w} = 0$ on $\partial(P \cap \tilde{P}) - \partial\Omega$. Suppose $P - \tilde{P}$ has positive Hausdorff measure. Then, since w satisfies homogeneous boundary conditions on $\partial(P - \tilde{P})$ and $\Delta w = 0$ in $P - \tilde{P}$, we deduce $w = 0$ in $P - \tilde{P}$. The unique continuation of harmonic functions implies then $w = 0$ in P and consequently also $w = 0$ on Γ_1, which contradicts the Dirichlet boundary condition (5.25). I.e., $P - \tilde{P}$ has Hausdorff measure 0 and in an analogous way we show that $\tilde{P} - P$ is of zero measure. Thus, we obtain $\Gamma = \tilde{\Gamma}$. □

5.3.2 Zero Space Charge and Unipolarity

As explained in Section 4, we have $p = 0$ respectively $v = 0$ in the unipolar case, without loss of generality we assume that $\delta = 1$. In this case the direct problem reduces to

$$-\text{div } ((a + b\chi_N)\nabla\hat{u}) = 0 \qquad \text{in } \Omega \tag{5.27}$$

$$\hat{u} = 0 \qquad \text{on } \Gamma_1 \tag{5.28}$$

$$\hat{u} = 1 \qquad \text{on } \Gamma_0 \tag{5.29}$$

$$\frac{\partial\hat{u}}{\partial\nu} = 0 \qquad \text{on } \partial\Omega_N. \tag{5.30}$$

The measurement is given by $g_C = (a+b)\mu_n \frac{\partial \hat{u}}{\partial \nu}$ on Γ_1. This problem is usually called *inverse conductivity problem*, it is well-known that it is exponentially ill-posed, too. In this case only local identifiability can be shown. (cf. [4, 24, 35]), i.e., the parameters are determined uniquely by the data only in a sufficiently small neighborhood of a solution. Global uniqueness can be shown only for severe and rather unrealistic restrictions on the parameter, e.g. if the junction is a closed inner curve and the enclosed set is a convex polyhedron (cf. [24]).

6 Regularization of the Inverse Problem

In this section we discuss the stable solution of the inverse doping problems. In the preceding sections we have seen that the doping profile does not depend on the data in a stable way, in some special cases we found that it is severely ill-posed, e.g. for the unipolar problem or the limit of zero space charge and low injection discussed in Section 5.3.1, where only logarithmic or even doubly logarithmic stability estimates hold for the identification problem under reasonable smoothness conditions.

We shall denote the exact data by Y and the noisy data by Y^δ and assume that the data error is bounded by

$$\left\| Y - Y^\delta \right\| \leq \delta. \tag{6.1}$$

The parameter-to-output map will be denoted by F in the following, which allows us to write all inverse doping problems in the abstract form

$$F(C) = Y^\delta. \tag{6.2}$$

Due to the ill-posedness of the inverse problem and the fact that one has noise in the data caused by measurement errors, one cannot use a standard iterative method for the solution of equation (6.2), since this would lead to a strong amplification of the noise. For implicit methods like the classical Gauss-Newton iteration

$$F'(C_k)^* F'(C_k)(C_{k+1} - C_k) = -F'(C_k)^*(F(C_k) - Y^\delta) \tag{6.3}$$

one cannot even guarantee the well-definedness of the iteration procedure, since the inverse of $F'(C_k)^* F'(C_k)$ need not exist and if it exists, it may be unstable. Therefore so-called *regularization methods* have to be used in order to obtain a stable approximation to the solution of equation (6.2) also in the presence of noise. A classical and popular method is *Tikhonov regularization*, where a regularized solution C_α^δ is a minimizer over $\mathcal{D}$ of the functional

$$C \mapsto \left\| F(C) - Y^\delta \right\|^2 + \alpha \left\| C - C_* \right\|^2_{L^2(\Omega)} \tag{6.4}$$

with $\alpha > 0$ chosen in dependence of the noise level δ and possibly also of the noisy data Y^δ. The function $C_* \in \mathcal{D}$, which appears in the second part of the functional in (6.4) is a given prior, such that a-priori information about the solution can be incorporated. If the solution of (6.2) for exact data is not unique, the second term will favor the one with minimal distance to the prior C_*. Although a comprehensive convergence analysis is available (cf. [18, 19, 46]), Tikhonov regularization has the serious disadvantage that one has to determine a global minimizer of the functional in (6.4), which is in general not convex for nonlinear problems and might have many local minima, which presents numerical difficulties. However, Tikhonov regularization has been applied with some success to electrical impedance tomography (cf. [17, 42]) and might therefore be of interest for inverse doping problems, too.

An alternative to Tikhonov regularization are *iterative regularization methods*, where the main regularizing effect comes from an early termination of the iteration procedure. The stopping index k_* is chosen dependent on the noise; a well-investigated and easy implementable rule for the choice of k_* is the so-called *generalized discrepancy principle* according to which k_* should be chosen such that

$$\left\| F(C_{k_*}) - Y^\delta \right\| \leq \tau\delta < \left\| F(C_k) - Y^\delta \right\|, \qquad \forall\, k < k_*, \tag{6.5}$$

for appropriately chosen $\tau > 1$. The motivation for this principle is that one has no criterion to compare the quality of iterates yielding a residual less than the noise level, since also the exact solution might yield a residual of this order, and therefore one should stop the iteration the first time the residual is of the same size as the noise level. Possibly the simplest iterative regularization method is the so-called *Landweber iteration*

$$C_{k+1}^\delta = C_k^\delta - F'(C_k^\delta)^*(F(C_k^\delta) - Y^\delta), \tag{6.6}$$

a rather slow but stable fixed-point iteration. The convergence analysis of this method with the generalized discrepancy principle as the stopping rule has been carried out by Hanke et. al. [28]; the type of convergence we can expect is convergence of C_k to a solution $\overline{C}$ of (6.2) in the case of exact data. In presence of noise, the convergence result is $C_{k_*}^\delta \to \overline{C}$ as $\delta \to 0$, i.e., the regularized approximations converge to a solution as the noise level tends to zero. If the solution of (6.2) is nonunique, then $\overline{C}$ will be the solution of minimal distance to the initial value C_0.

Faster iterative methods are modifications of the Gauss-Newton iteration such as the *Levenberg-Marquardt iteration* (cf. [27])

$$C_{k+1}^\delta = C_k^\delta - (F'(C_k^\delta)^* F'(C_k^\delta) + \alpha_k I)^{-1} F'(C_k^\delta)^*(F(C_k^\delta) - Y^\delta), \tag{6.7}$$

or the *iteratively regularized Gauss-Newton method* (cf. [7, 32])

$$C_{k+1}^\delta = C_k^\delta - (F'(C_k^\delta)^* F'(C_k^\delta) + \alpha_k I)^{-1} \left(F'(C_k^\delta)^*(F(C_k^\delta) - Y^\delta) + \alpha_k (C_k^\delta - C_0) \right), \tag{6.8}$$

with $\alpha_k > 0$. Both are based on a Tikhonov-type stabilization of the linearized problem (6.3), where the prior is C_k^δ for the Levenberg-Marquardt iteration and C_0 for the iteratively regularized Gauss-Newton method. Due to the fixed prior in the latter it is necessary that α_k tends to zero with increasing iteration index k, while for the Levenberg-Marquardt method this parameter could also be chosen constant during the iteration.

The convergence analysis of Newton-type methods shows that we may expect to be faster than the Landweber iteration, since the number of iterations needed until the stopping criteria is satisfied is lower. However, this advantage is often compensated by a higher effort in each iteration step, which will be explained in the next Section. For a more detailed exposition of iterative regularization methods for inverse problems we refer to [16, 18, 20].

6.1 Iterative Regularization of Inverse Doping Problems

For the application of iterative regularization to inverse doping problems we need the first derivative of the parameter-to-output map and its adjoint. For the sake of simplicity we restrict ourselves to the case of reduced voltage-current data, but an analogous treatment is possible for all other cases, too.

In order to compute the derivative of the parameter-to-output map G, we denote by $(\hat{u}_j, \hat{v}_j)$ the solution of (3.11)-(3.13) with particular Dirichlet value $\Phi = U_j$. The formal linearization of (3.11)-(3.13) with respect to a variation of C in direction h is the system

$$\operatorname{div}\ \left(\mu_n e^V (\nabla \phi_j + \theta \nabla \hat{u}_j)\right) = Q_0(V,x)(\phi_j + \psi_j) + \left(Q_0'(V)\theta\right)(\hat{u}_j + \hat{v}_j) \quad \text{in } \Omega \tag{6.9}$$

$$\operatorname{div}\ \left(\mu_p e^{-V} (\nabla \psi_j - \theta \nabla \hat{v}_j)\right) = Q_0(V,x)(\phi_j + \psi_j) + \left(Q_0'(V)\theta\right)(\hat{u}_j + \hat{v}_j) \quad \text{in } \Omega \tag{6.10}$$

$$\phi_j = \psi_j = 0 \quad \text{on } \partial\Omega_D \tag{6.11}$$

$$\frac{\partial \phi_j}{\partial \nu} = \frac{\partial \psi_j}{\partial \nu} = 0 \quad \text{on } \partial\Omega_N. \tag{6.12}$$

for (ϕ, ψ), where θ is the solution of the linearized equilibrium problem

$$\lambda^2 \Delta \theta = (e^V + e^{-V})\theta - h \quad \text{in } \Omega \tag{6.13}$$

$$\theta = 0 \quad \text{on } \partial\Omega_D \tag{6.14}$$

$$\frac{\partial \theta}{\partial \nu} = 0 \quad \text{on } \partial\Omega_N. \tag{6.15}$$

The linearization of the nonlinear operator G can now be written in terms of (ϕ_j, ψ_j) as

$$\begin{array}{rccc} G'(C)h: & L^2(\Omega) & \to & L^2(\Gamma_1)^N \\ & h & \mapsto & \left(Z_j'\right)_{j=1,\dots,N}, \end{array} \tag{6.16}$$

where Z_j' is the output of the pair (ϕ_j, ψ_j), i.e.,

$$Z_j' = \left(\mu_n e^V \phi_j - \mu_p e^{-V} \psi_j\right)|_{\Gamma_1}. \tag{6.17}$$

We note that θ does not appear explicitly in the output Z_j' because it satisfies a homogeneous Dirichlet boundary condition on $\partial\Omega_D \supset \Gamma_1$ and therefore the variation of the output with respect to V in direction θ is zero.

The above computation of the derivative of $G'(C)$ shows that we have to solve first the linearized equilibrium problem (6.13)-(6.15) to obtain the map $h \mapsto \theta$ and then solve the N elliptic systems (6.9)-(6.12), which yields the second step $\theta \mapsto \{(\phi_j, \psi_j)\}_{j=1,\dots,N}$. Finally, we have to evaluate the trace-type map (6.17) for each of the N solution pairs to obtain the output $(Z_j')_{j=1,\dots,N}$.

This means that the use of a Newton-type method for the solution of the inverse doping problem would cause an enormous numerical effort in each iteration step, since we have to evaluate the derivative of the parameter-to-output map G several times in order to assemble the Newton matrix. Therefore we turn our attention to the Landweber iteration in the following, where it suffices to evaluate the adjoint of $G'(C)$ once in each iteration step and where one does not need to solve a linear system of large scale as in the Newton step. Since the evaluation of the adjoint is usually even of less effort than the evaluation of $G'(C)$ itself, the Landweber iteration is often more efficient than a Newton-type iteration although the number of iterations needed is much higher. This statement holds in particular for large scale problems and has been confirmed by the results for some identification problems in practical applications (cf. e.g. [11, 12, 13]).

The computation of the adjoint of the derivative, which is needed for an implementation of the Landweber iteration will be explained in detail in Section 7.

6.2 Rate of Convergence

In order to obtain convergence rates of regularization methods for inverse problems, additional assumptions on the solution, so-called *source conditions*, are needed. Classical source conditions are of the form

$$\exists\, w: \qquad C - C_0 = (F'(C)^* F'(C))^\nu w \tag{6.18}$$

for the solution C of (6.2) and some $\nu > 0$. Such source conditions are abstract smoothness conditions on the difference between the solution and the initial guess C_0, where the degree of smoothness increases with ν. However, for exponentially ill-posed problems such as inverse scattering or impedance tomography, such conditions turned out to be by far too restrictive, in many cases not even analyticity of $C - C_0$ is sufficient (cf. [30, 31] for further details). Therefore, so-called *logarithmic source conditions* have been introduced to obtain reasonable smoothness conditions. A logarithmic source condition is of the form

$$\exists\, w: \qquad C - C_0 = f_\nu(F'(C)^* F'(C))w, \tag{6.19}$$

where the function f_ν is defined by

$$f_\nu(t) = \begin{cases} (\ln e - \ln t)^{-\nu} & \text{for } 0 < t < 1 \\ 0 & \text{else} \end{cases} \tag{6.20}$$

for some $\nu > 0$. It has been shown that under condition (6.19) the rate result

$$\left\| C - C_{k_*}^\delta \right\| = \mathcal{O}\left((-\ln\delta)^{-\nu}\right) \tag{6.21}$$

$$k_* = \mathcal{O}\left(\frac{(-\ln\delta)^{-2\nu}}{\delta^2}\right) \tag{6.22}$$

holds for the Landweber iteration with stopping index chosen according to the generalized discrepancy principle (6.5) (cf. [16, Theorem 2.8 and Lemma A.6]).

Since for our inverse problems, we can at best expect logarithmic stability estimates under reasonable smoothness conditions (cf. Sections 4 and 5), logarithmic source conditions and hence logarithmic convergence rates will have to be expected for Landweber iteration.

7 Numerical Solution

In this section we want to discuss the numerical solution of the inverse doping problem in a particular application. As an obvious starting example we consider the p-n diode in the limiting case of zero space charge and low injection as discussed in Section 5.3.1, restricting ourselves to the important case $\Omega \subset \mathbf{R}^2$. The geometry of the diode is a square with length $L = 10^{-4}m$. The contact Γ_1, at which the measurement of the current density is taken, is located at the top of the device and has a length of $2.5 * 10^{-5}m$; the second contact is at the bottom and ranges over the full length of 10^{-4} (see Figure 3). The doping profile to be reconstructed is of the form

$$C \quad = \quad \begin{cases} -C_0 & \text{in } P, \\ C_0 & \text{in } N, \end{cases} \tag{7.1}$$

where the P-region is the quarter of a circle with radius $r = 5 * 10^{-5}m$, whose center is located at the left upper corner of the device (see Figure 3). We want to identify the curve Γ separating the P- and N-region. The material parameters we use are taken from silicon at room temperature and listed in Table 1.

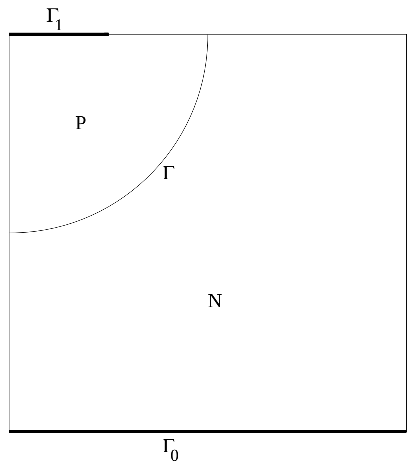

Figure 3: Geometry of the p-n diode with the contacts Γ_0 and Γ_1 and the junction Γ.

Parameter	**Symbol**	**Value**
Permittivity	ϵ_s	10^{-10} AsV^{-1}m^{-1}
Elementary charge	q	10^{-19} As
Thermal voltage	U_T	$2.5 * 10^{-2}$ V
Intrinsic density	n_i	10^{16} m^{-3}
Electron mobility	μ_n	10^{-1} m^{2}V^{-1}s^{-1}
Hole mobility	μ_p	10^{-1} m^{2}V^{-1}s^{-1}

Table 1: Material parameters for silicon.

7.1 Parameterization of Γ

We assume that the domain P is star-shaped with respect to the left upper corner point of the device, the curve Γ can be parameterized in this case by

$$\Gamma = \left\{ r(\theta)(\cos\theta, -\sin\theta) \mid \theta \in [0, \frac{\pi}{2}] \right\}, \tag{7.2}$$

where r denotes the distance of the point on the curve from the left corner on top of the device. In a first numerical example we therefore try to identify the function $r \in H^1([0,\pi/2])$ from voltage-current measurements in the case of low injection and zero space charge. After appropriate rescaling, we can replace the current density data by $\frac{\partial \hat{u}}{\partial \nu}|_{\Gamma_1}$, where $\hat{u}$ is the solution of the boundary value-problem (5.14)-(5.17).

The parameter-to-output map can be defined also in terms of the parameterization r, i.e.,

$$\begin{aligned} F: \quad H^1([0,\pi/2]) &\rightarrow L^2(\Gamma_1) \\ r &\mapsto \tfrac{\partial \hat{u}}{\partial \nu}|_{\Gamma_1}, \end{aligned} \tag{7.3}$$

where $\hat{u}$ is the solution of the Laplace-equation (5.14) in P supplemented by the boundary conditions (5.15)-(5.17). The evaluation of the parameter-to-output map for a certain r consists in solving the Laplace equation in the domain $P(r)$ with the boundary curve $\Gamma(r)$ defined via (7.2) and subsequent evaluation of the normal derivative $\frac{\partial \hat{u}}{\partial \nu}$ on the contact Γ_1. The derivative of this map is given by

$$F'(r)\rho = \frac{\partial w}{\partial \nu}|_{\Gamma_1}, \tag{7.4}$$

where w is the solution of the boundary value problem

$$-\Delta w = 0 \qquad \text{in } P(r) \tag{7.5}$$

$$w = -\frac{\rho}{r}\nabla \hat{u}.x \qquad \text{on } \Gamma(r) \tag{7.6}$$

$$w = 0 \qquad \text{on } \Gamma_1 \tag{7.7}$$

$$\frac{\partial w}{\partial \nu} = 0 \qquad \text{on } \partial\Omega_N \cap \partial P(r) \tag{7.8}$$

We want to reconstruct r using the Landweber iteration

$$r_{k+1}^\delta = r_k^\delta - F'(r_k^\delta)^*(F(r_k^\delta) - g^\delta), \tag{7.9}$$

where g^δ are the (noisy) measurements for $\frac{\partial \hat{u}}{\partial \nu}$ on Γ_1. The numerical implementation of the Landweber iteration enforces the evaluation of the forward operator F, which was described above, and the evaluation of the adjoint $F'(r)^*h$. In order to compute the latter we define an *adjoint problem* by

$$-\Delta w^* = 0 \qquad \text{in } P(r) \tag{7.10}$$

$$w^* = 0 \qquad \text{on } \Gamma(r) \tag{7.11}$$

$$w^* = h \qquad \text{on } \Gamma_1 \tag{7.12}$$

$$\frac{\partial w^*}{\partial \nu} = 0 \qquad \text{on } \partial\Omega_N \cap \partial P(r). \tag{7.13}$$

By applying Gauss' Theorem and inserting the equations for w and w^* we obtain

$$\begin{aligned}
\langle F'(r)\rho, h\rangle &= \int_{\Gamma_1} \frac{\partial w}{\partial \nu}\, h \, d\sigma = \int_{\Gamma_1} \frac{\partial w}{\partial \nu}\, w^* \, d\sigma \\
&= \int_{P(r)} (\nabla w . \nabla w^* - (\Delta w) w^*) \, dx - \int_{\Gamma(r)} \frac{\partial w}{\partial \nu}\, w^* \, d\sigma \\
&= -\int_{P(r)} w \Delta w^* \, dx + \int_{\Gamma(r)} w \frac{\partial w^*}{\partial \nu} \, d\sigma \\
&= -\int_{\Gamma(r)} \frac{\rho}{r} (x.\nabla \hat{u}) \frac{\partial w^*}{\partial \nu} \, d\sigma.
\end{aligned}$$

Because of

$$\frac{d\sigma}{d\theta} = \sqrt{\dot{r}(\theta)^2 + r(\theta)^2},$$

we may perform a change of variables in the last integral to deduce

$$\langle F'(r)\rho, h\rangle = -\int_0^{\frac{\pi}{2}} \rho \nabla \hat{u}.(\cos\theta, -\sin\theta) \frac{\partial w^*}{\partial \nu} \sqrt{\dot{r}^2 + r^2}\, d\theta.$$

We note that so far we have formally computed the adjoint with respect to the scalar product of $L^2([0, \pi/2])$, which is given by

$$F'(r)^*_{L^2} h = -\nabla \hat{u}.(\cos\theta, -\sin\theta) \frac{\partial w^*}{\partial \nu} \sqrt{\dot{r}^2 + r^2}. \tag{7.14}$$

Since it involves the derivative $\dot{r}$ of r with respect to θ, which need not exist on $L^2([0, \pi/2])$, it is well-defined only for $r \in H^1([0, \pi/2])$. To complete the derivation of the adjoint in $H^1([0, \pi, 2])$, we only need to apply the adjoint of the embedding operator from $L^2([0, \pi/2])$ to $H^1([0, \pi/2])$. I.e., the adjoint $F'(r)^*$ is given by $F'(r)^* h = f$, where $f \in H^1_0([0, \pi, 2])$ solves

$$\frac{d^2 f}{d\theta^2} - f = \nabla \hat{u}.(\cos\theta, -\sin\theta) \frac{\partial w^*}{\partial \nu} \sqrt{\dot{r}^2 + r^2}, \tag{7.15}$$

since

$$\begin{aligned}
\langle \rho, F'(r)^* h\rangle_{H^1} &= \int_0^{\frac{\pi}{2}} \left(\frac{d\rho}{d\theta}\frac{df}{d\theta} + \rho\, f \right) d\theta \\
&= \int_0^{\frac{\pi}{2}} \rho \left(-\frac{d^2 f}{d\theta^2} + f \right) d\theta,
\end{aligned}$$

and the last term equals $\langle F'(r)\rho, h\rangle$ due to (7.15) and the above derivation of the adjoint in $L^2([0, \pi/2])$.

As one observes from (7.10)-(7.13), the main part in the evaluation of the adjoint is to solve a system that differs from the forward problem only by changes in the right-hand side. Therefore we can use the same solvers and the same meshing for the forward and the adjoint problems. The remaining part of computing the term (7.14) can be realized with small extra effort, since the solutions $\hat{u}$ and w^* of the forward and the adjoint problems have been computed anyway.

The discretization of the problem is performed in two steps; first we discretize the boundary Γ via linear splines, which connect the corner points

$$(r(\theta_j)(\cos\theta_j, -\sin\theta_j))_{j=0,\ldots,M},$$

where $0 = \theta_0 < \theta_1 < \ldots < \theta_M = \frac{\pi}{2}$ is an appropriate discretization of the parameter θ. The second step is to assemble a triangular mesh on the corresponding domain $P(r)$, on which we use linear conforming finite elements to solve the Laplace equation with boundary conditions (5.15)-(5.17) to obtain $\hat{u}$ and with boundary conditions (7.11)-(7.13) to obtain the solution w of the adjoint problem. The remaining parts of evaluating the output $\frac{\partial \hat{u}}{\partial \nu}|_{\Gamma_1}$ and the update in r^k can be performed by standard methods on the one-dimensional manifolds Γ_1 and Γ. We note that the assembly of a new mesh in each iteration step leads to considerable numerical effort. A possible alternative would be a transformation of the mesh from the previous domain $P(r_{k-1})$ to the new domain $P(r_k)$, but this can lead to triangles that do not satisfy the standard regularity conditions for a finite element mesh.

7.2 Numerical Results

For the numerical simulation of the inverse boundary problem for the equation (5.14)-(5.17), we used two different types of data:

1. For a test of our reconstruction algorithm and numerical investigations of the stability we use data generated using directly the model (5.14)-(5.17) perturbed by artificial noise, but with a different discretization than in the reconstruction algorithm in order to avoid 'inverse crimes', which would amount to generate data and to solve the problem in the same finite-dimensional subspace, thus eliminating the ill-posedness in an inappropriate way.

2. For a verification that the reconstruction of the junction via the reduced model (5.14)-(5.17) can successfully replace the reconstruction via the full drift-diffusion model, we use data generated by solving the drift-diffusion equations such that the limiting conditions on the parameters are satisfied, i.e.,

$$\lambda, \delta << 1 \qquad \text{and} \qquad \lambda^2 \log(\delta^{-2}) << 1 \tag{7.16}$$

   (cf. [40]). Since the methods and discretizations for generating the data and for solving the inverse problem are completely different, this obviously cannot cause inverse crimes. Our goal is to confirm that for the solution of the inverse problem with the reduced model, the data from the drift-diffusion model are of the same quality as noisy data from the reduced model.

For all test cases we used the Landweber iteration with the numerical algorithms described above.

Data from the Reduced Model

For the data from the reduced model we used a scaling of the doping profile of the size $C_0 = 10^{20} m^{-3}$, which is a realistic size for silicon diodes. The output current density, which has been generated by solving the reduced model (5.14)-(5.17), is perturbed by artificial noise

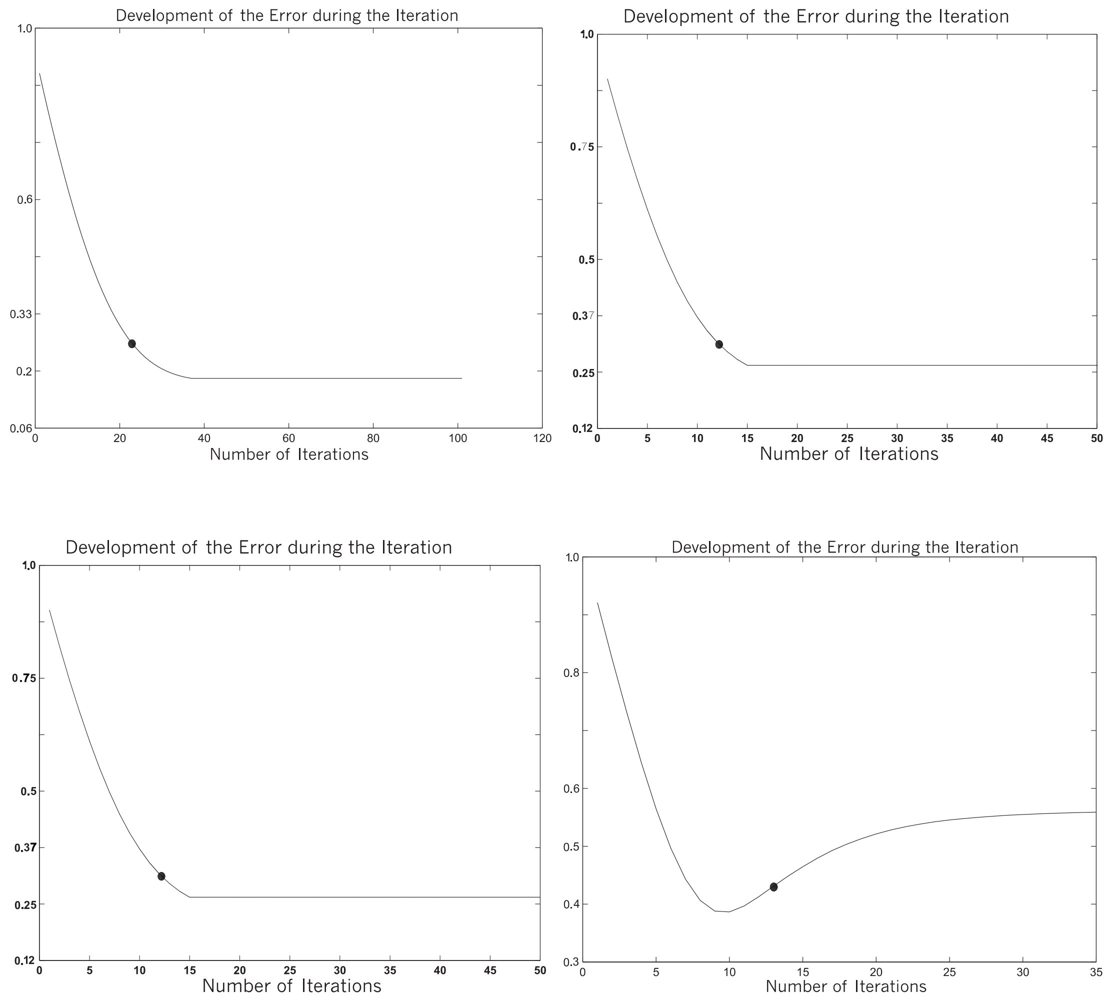

Figure 4: Evolution of the error between reconstruction and exact junction during the iteration, for $\delta = 2.5\%$ (above left), $\delta = 5\%$ (above right), $\delta = 7.5\%$ (below left) and $\delta = 10\%$ (below right). The stopping index obtained with the generalized discrepancy principle is marked by a circle.

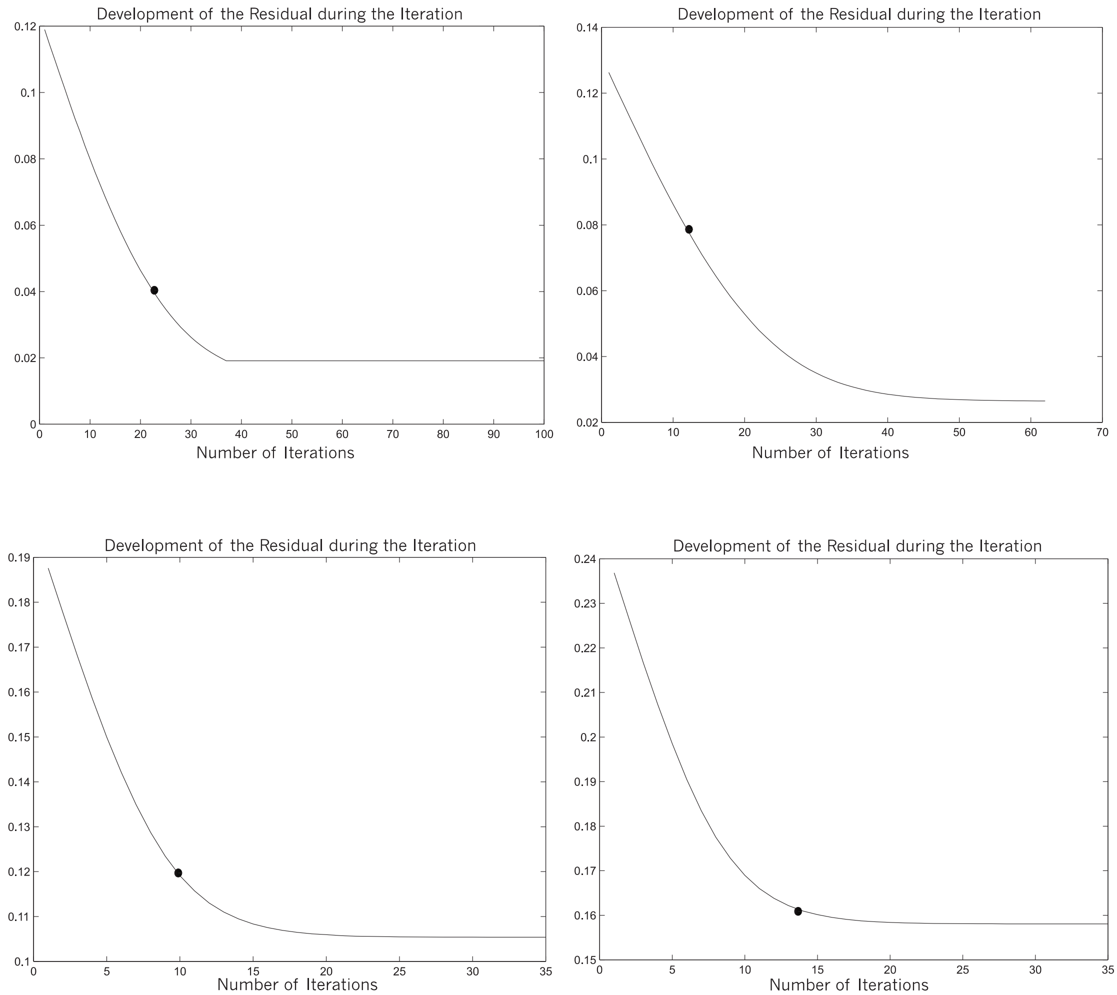

Figure 5: Evolution of the residual during the iteration, for $\delta = 2.5\%$ (above left), $\delta = 5\%$ (above right), $\delta = 7.5\%$ (below left) and $\delta = 10\%$ (below right). The stopping index obtained with the generalized discrepancy principle is marked by a circle.

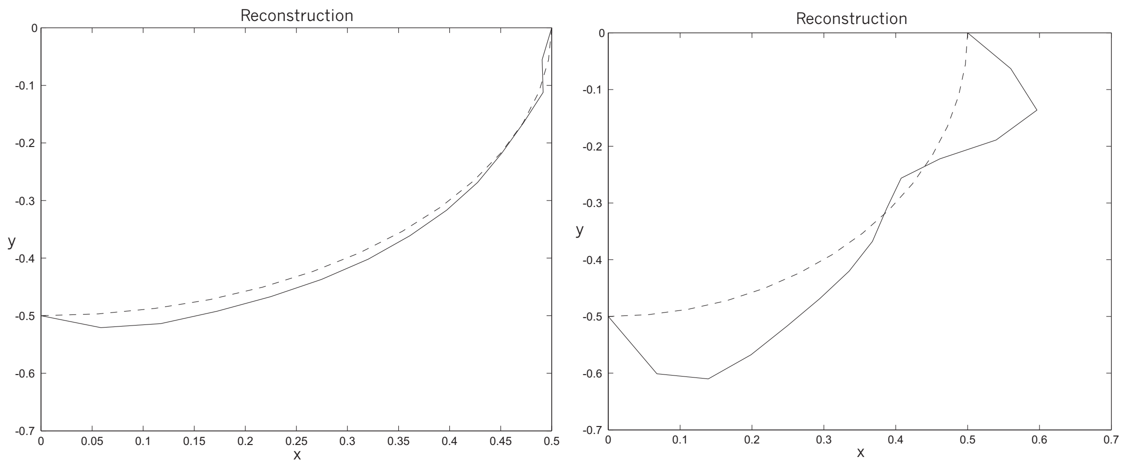

Figure 6: Reconstruction using noisy data from the reduced model for noise levels $\delta = 2.5\%$ (left) and $\delta = 10\%$ (right) compared to the exact junction (dotted).

of high frequency, which allows to verify the regularization behavior since we know the size of δ. In particular, this allows to choose the stopping index according to the generalized discrepancy principle (6.5), for which we chose a fixed parameter τ.

We discuss the behavior of the Landweber iteration for different noise levels, in particular for $\delta = 2.5\%$, $\delta = 5\%$,$\delta = 7.5\%$ and $\delta = 10\%$, which is shown in Figures 4-6. The evolution of the error between the exact junction Γ and the junction Γ_k obtained during the Landweber iteration is shown in Figure 4, one observes that the error is decreasing significantly farther in the case of less noise. In addition, the instability, which causes the error to increase after some iterations, occurs later in the case of smaller noise level (see Figure 4), which is a typical effect for (severely) ill-posed problems. The residual $\left\|F(r_k^\delta) - g^\delta\right\|$ has a similar behavior during the iteration, with the difference that it always decreases (although very slow after some iterations). This confirms the usual principle of choosing the stopping index not according to the change of the residual or the approximations in two consecutive steps as for well-problems, but by the generalized discrepancy principle (6.5), which only uses the actual size of the residual compared to the noise level.

The quality of the reconstructions is shown in Figure 6, they clearly depend strongly on the noise level, which can be observed by a comparison of the reconstruction for $\delta = 2.5\%$ and $\delta = 10\%$. The reconstructed junction for 2.5% is much closer to the exact one than the one with 10% and appears to be more regular, which is another consequence of smaller noise levels. We will see below that similar effects appear if data generated with the drift-diffusion model are used.

Data from the Drift-Diffusion Model

For the data generated with the drift-diffusion model, we used a well-known exponential fitting scheme for the continuity equations, which is based on a discretization of the saddle-point formulation by mixed finite elements (cf. [8] for further details). We used two doping profiles of the same shape, but of different sizes, namely $C_0 = 10^{20} m^{-3}$ and $C_0 = 10^{21} m^{-3}$; the applied voltage was $U = 0.3V$. We note that in this case we need not compute the data

$\mathbf{C_0}$	λ^2	δ^2	$\lambda^2 \log(\delta^{-2})$
$10^{20}m^{-3}$	$2.5 * 10^{-5}$	10^{-4}	10^{-4}
$10^{21}m^{-3}$	$2.5 * 10^{-6}$	10^{-5}	$1.25 * 10^{-5}$

Table 2: Parameter values for the different sizes of the doping profile.

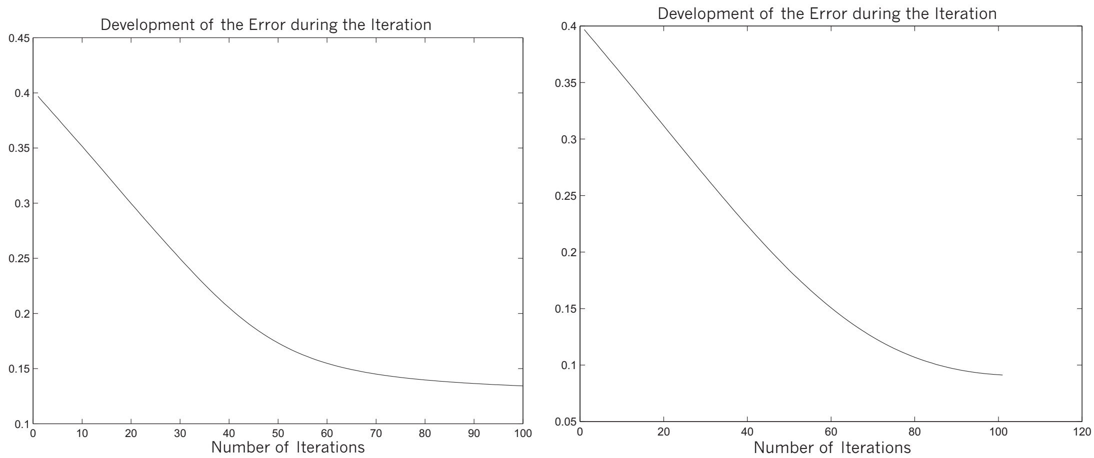

Figure 7: Evolution of the error between reconstruction and exact junction during the iteration, for $C_0 = 10^{20}m^{-3}$ (left) and $C_0 = 10^{21}m^{-3}$ (right)

g_C by numerical differentiation (as one would have to in general), since the functions u and $\hat{u}$ are related by (5.12), i.e., we have

$$\frac{\partial \hat{u}}{\partial \nu}|_{\Gamma_1} \approx \frac{1}{e^U - 1}\frac{\partial u}{\partial \nu}|_{\Gamma_1}$$

in the case of "small space-charge" and low injection (which we consider here).

The resulting values of the parameters λ and δ are given in Table 2; the output for these cases of parameters can also be interpreted as two different cases of noisy data for the reduced model. Since the characteristic parameter values (λ^2 and $\lambda^2 \log(\delta^{-2})$) are smaller in the second setup, the approximation of the reduced model to the drift-diffusion equations should be better in this case and therefore we can interpret it as the case with 'smaller noise level' for the reduced model. This interpretation is very well confirmed by the numerical results shown in Figures 7-9. Figure 7 shows the evolution of the error between the exact junction and the reconstruction during the iteration procedure; one observes that in the case of larger C_0 the error decreases over a longer period, which usually indicates less noise (see also Figure 4) and therefore confirms the interpretation of small λ and δ (respectively large C_0) as small noise level for the reduced model. In addition, the minimal error obtained in the second case is significantly smaller, which is a typical feature for reconstructions with smaller noise level.

Figure 8 shows the evolution of the residual $\|F(r_k) - g\|$ during the iteration, which is farther decreasing in the case of larger C_0 and therefore confirms the interpretation of lower noise. Finally, the reconstructions that yield the smallest residual are shown in Figure 9, one can observe that their visual quality is not of the same quality as for the ones in Figure 6 with

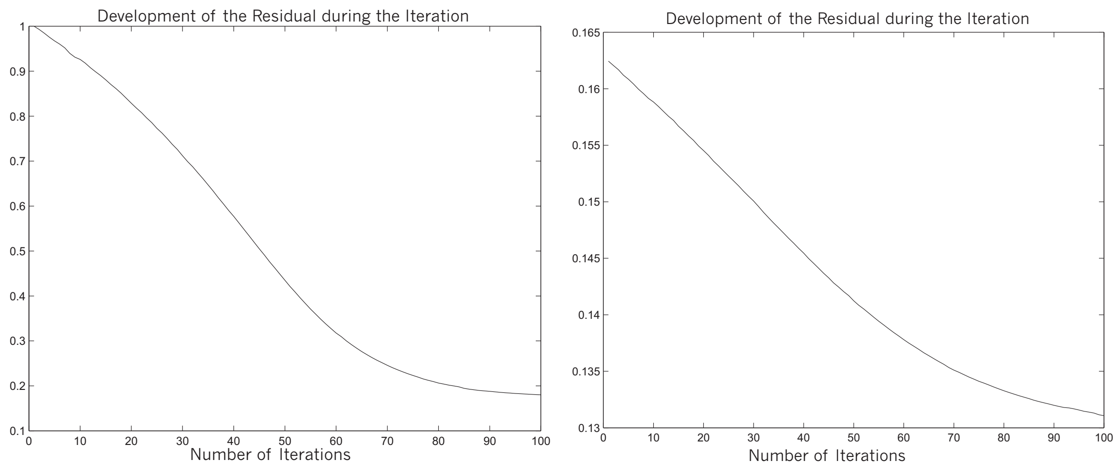

Figure 8: Evolution of the residual during the iteration, for $C_0 = 10^{20}m^{-3}$ (left) and $C_0 = 10^{21}m^{-3}$ (right)

small noise level, but a comparison with the result obtained with 10% noise indicates that the 'artificial' noise caused by the use of the reduced model in the reconstruction is below this level.

8 Conclusions and Future Work

The framework for inverse doping problems developed above yields a variety of challenging subproblems and mathematical questions. The special cases obtained from scaling limits fall into better investigated classes of inverse problems; they are known to be difficult to solve and to be severely ill-posed. The more general cases are even more complex and therefore a lot of future work will be necessary on this topic.

The theoretical and numerical results indicate that the amount of the data used here seems to be really necessary to identify doping profiles and therefore approaches using less information are most likely not able to yield reasonable reconstructions. On the other hand, using this amount of data we have obtained good numerical results in spite of the (also demonstrated) ill-posedness of the problem. Possibly the kind of data we use for the identification can be obtained also under industrial conditions in the near future due to the strong technological progress in this area. In addition to our investigations close to equilibrium it would be of interest to explore possible data far away from equilibrium, which includes many important theoretical and numerical problems that have not been solved so far.

A wide field for future work is the development of numerical methods for inverse doping problems considered in this paper and the application to more advanced semiconductor devices, in particular to MOSFETs (cf. [40] for a detailed description). We have solved only a special case of lower complexity, but already there we encountered an inverse problem, whose numerical solution required a considerable effort. Hence, special focus should be laid on the efficiency of the numerical solution methods. On the other hand, one prefers reconstruction algorithms, where existing solvers for the drift-diffusion equations can be used as black-box methods, since their development is very time-consuming due to the many non-standard tech-

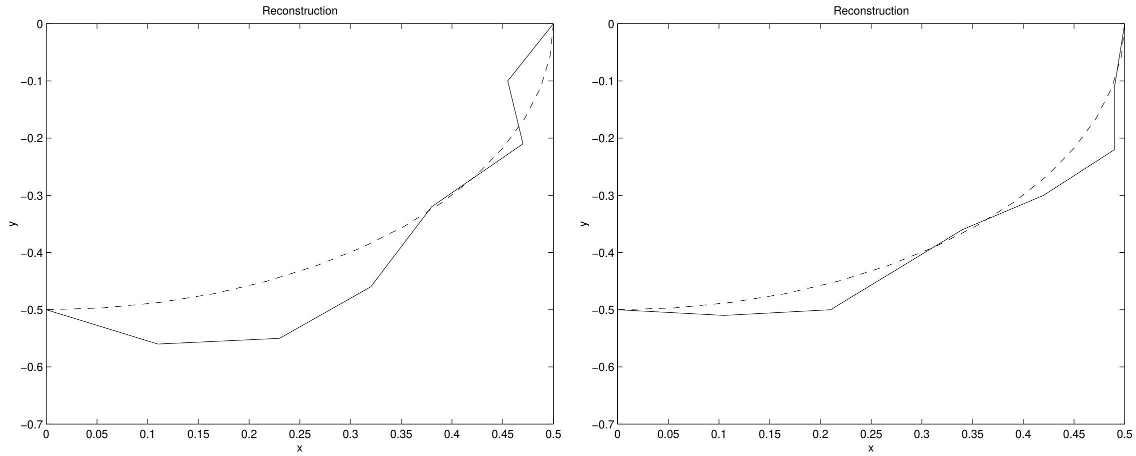

Figure 9: Reconstruction using data from the full drift-diffusion model for $C_0 = 10^{20} m^{-3}$ (left) and $C_0 = 10^{21} m^{-3}$ (right) compared to the exact junction (dotted).

niques that are necessary for good numerical approximations. It is not obvious at present if both criteria can be satisfied by a solution method for inverse doping problems or for optimal control problems related to the drift-diffusion model, where analogous numerical methods are needed (cf. [29]).

Another interesting problem for the future work is the identification of doping profiles in the transient drift-diffusion equations, which consist of the coupled elliptic-parabolic system

$$
\begin{aligned}
0 &= \operatorname{div}(\epsilon_s \nabla V) - q(n - p - C) && \text{in } \Omega \times (0,T) \\
\frac{\partial n}{\partial t} &= \operatorname{div}(D_n \nabla n - \mu_n n \nabla V) && \text{in } \Omega \times (0,T) \\
\frac{\partial p}{\partial t} &= \operatorname{div}(D_p \nabla p + \mu_p p \nabla V) && \text{in } \Omega \times (0,T)
\end{aligned}
$$

supplemented by appropriate initial and boundary conditions. In this case data can either be measured during a time interval $(0,T)$ or at the final time T. For the transient problem, global existence and uniqueness results are available (cf. [25, 45]) as well as results about the linearized problem (cf. [39]) and hence, the voltage-current map is well-defined for arbitrary applied voltages, which is a theoretical advantage over the stationary case.

Acknowledgments

This work has been supported by the Austrian National Science Foundation FWF under project grants SFB F 013 / 08 and P 13478-INF, by the EU under the TMR Network *Asymptotic Methods in Kinetic Theory*, grant number ERB-FMBX-CT97-0157, and by the Italian-Austrian technical scientific collaboration agreement. The third author acknowledges support from the Austrian National Science Foundation through his Wittgenstein Award.

References

[1] G.Alessandrini, *Stable determinations of conductivity by boundary measurements*, Appl. Anal. **27** (1988), 153-172.

[2] G. Alessandrini, *Singular solutions of elliptic equations and the determination of conductivity by boundary measurements*, J. Differential Equations **84** (1990), 252-272.

[3] G.Alessandrini, E.Beretta, E.Rosset, S.Vessella, *Optimal stability for elliptic boundary value problems with unknown boundaries*, Ann. Scuola Norm. Sup. Pisa (2000), to appear.

[4] G.Alessandrini, V.Isakov, J.Powell, *Local uniqueness in the inverse conductivity problem with one measurement*, Trans. Am. Math. Soc. **347**, (1995), 3031-3041.

[5] N.D.Aparicio, M.K.Pidcock, *The boundary inverse problem for the Laplace equation in two dimensions*, Inverse Problems **12** (1996), 565-577.

[6] E.Beretta, S.Vessella, *Stable determination of boundaries from Cauchy data*, SIAM J. Math. Anal. **30** (1998), 220-232.

[7] B.Blaschke(-Kaltenbacher), A.Neubauer, O.Scherzer, *On convergence rates for the iteratively regularized Gauss-Newton method*, IMA J.Numer.Anal. **17** (1997), 421-436.

[8] F.Brezzi, L.D.Marini, P.Pietra *Two-dimensional exponential fitting and applications in drift-diffusion models*, SIAM J. Numer. Anal. **26** (1989), 1342-1355.

[9] R.M.Brown, G.A.Uhlmann, *Uniqueness in the inverse conductivity problem for nonsmooth conductivities in two dimensions*, Commun. Partial Differ. Equations **22** (1997), 1009-1027.

[10] A.L. Bukhgeim, J.Cheng, M.Yamamoto, *Stability for an inverse boundary problem of determining a part of a boundary*, Inverse Problems **15** (1999), 1021-1032.

[11] M.Burger, V.Capasso, H.W.Engl, *Inverse problems related to crystallization of polymers*, Inverse Problems **15** (1999), 155-173

[12] M.Burger, *Iterative regularization of a parameter identification problem occurring in polymer processing* SFB-Report 99-21 (University of Linz, 1999), and submitted.

[13] M.Burger, *Direct and Inverse Problems in Polymer Crystallization Processes* (PhD Thesis, University of Linz, 2000).

[14] S.Busenberg, W.Fang, *Identification of semiconductor contact resistivity*, Q. Appl. Math. **49** (1991), 639-649.

[15] M.Cheney, D.Isaacson, J.C.Newell, *Electrical impedance tomography*, SIAM Review **41** (1999), 85-101.

[16] P.Deuflhard, H.W.Engl, O.Scherzer, *A convergence analysis of iterative methods for the solution of nonlinear ill-posed problems under affinely invariant conditions*, Inverse Problems **14** (1998), 1081-1106.

[17] D.C.Dobson, *Convergence of a reconstruction method for the inverse conductivity problem*, SIAM J. Appl. Math. **52** (1992), 442-458.

[18] H.W.Engl, M.Hanke, A.Neubauer, *Regularization of Inverse Problems* (Kluwer, Dordrecht, 1996; paperback edition, 2000).

[19] H.W.Engl, K.Kunisch, A.Neubauer, *Convergence rates for Tikhonov regularisation of nonlinear ill-posed problems*, Inverse Problems **5** (1989), 523-540.

[20] H.W.Engl, O.Scherzer, *Convergence rate results for iterative methods for solving nonlinear ill-posed problems*, in D.Colton,H.W. Engl, A.Louis, J.McLauglin, W.Rundell, eds., *Surveys on Solution Methods for Inverse Problems* (Springer, Vienna, 2000).

[21] W.Fang, E.Cumberbatch, *Inverse problems for metal oxide semiconductor field-effect transistor contact resistivity*, SIAM J. Appl. Math. **52** (1992), 699-709.

[22] W.Fang, K.Ito, *Identifiability of semiconductor defects from LBIC images*, SIAM J. Appl. Math. **52** (1992), 1611-1626.

[23] W.Fang, K.Ito, *Reconstruction of semiconductor doping profile from laser-beam-induced current image*, SIAM J. Appl. Math. **54** (1994), 1067-1082.

[24] A.Friedman, V.Isakov, *On the uniqueness in the inverse conductivity problem with one measurement*, Indiana Univ. Math. J. **38** (1989), 563-579.

[25] H.Gajewski, *On existence, uniqueness and asymptotic behavior of solutions of the basic equations for carrier transport in semiconductors*,Z. Angew. Math. Mech. **65**, 101-108.

[26] D.Gilbarg, N.S.Trudinger, *Elliptic Partial Differential Equations of Second Order* (Springer, Berlin, Heidelberg, New York, 1977).

[27] M.Hanke, *A regularizing Levenberg-Marquardt scheme, with applications to inverse groundwater filtration problems*, Inverse Problems **13** (1997), 79-95.

[28] M.Hanke, A.Neubauer, O.Scherzer, *A convergence analysis of the Landweber iteration for nonlinear ill-posed problems*, Numer. Math. **72** (1995), 21-37.

[29] M. Hinze , R. Pinnau, *Optimal control of the drift-diffusion model for semiconductor devices* , Preprint Nr. 2118 (Technical University Darmstadt, 2000).

[30] T.Hohage, *Iterative Methods in Inverse Obstacle Scattering: Regularization Theory of Linear and Nonlinear Exponentially Ill-Posed Problems* (PhD Thesis, University of Linz, 1999).

[31] T.Hohage, *Regularisation of exponentially ill-posed problems*, Numer. Funct. Anal. Optim. **21** (2000), 439-464.

[32] B.Kaltenbacher, *Some Newton-type methods for the regularization of nonlinear ill-posed problems*, Inverse Problems **13** (1997), 729-753.

[33] N.Khalil, *ULSI Characterization with Technology Computer-Aided Design* (PhD-Thesis, Technical University Vienna, 1995).

[34] R.Kohn, M.Vogelius, *Determining conductivity by boundary measurements*, Commun. Pure Appl. Math. **37** (1984), 289-298.

[35] V.Isakov, J.Powell, *On the inverse conductivity problem with one measurement*, Inverse Problems **6**, 311-318 (1990).

[36] J.L.Lions, E.Magenes, *Non-Homogenous Boundary Value Problems and Applications, Vol. I* (Springer, Berlin, Heidelberg, New York, 1972).

[37] P.A.Markowich, *A singular perturbation analysis of the fundamental semiconductor device equations*, SIAM J. Appl. Math. **44** (1984), 896-928.

[38] P.A.Markowich, *The Stationary Semiconductor Device Equations* (Springer, Wien, New York, 1986).

[39] P.A.Markowich, C.A.Ringhofer, *Stability of the linearized transient semiconductor device equations*, Z. Angew. Math. Mech. **67** (1987), 319-332.

[40] P.A.Markowich, C.A.Ringhofer, C.Schmeiser, *Semiconductor Equations* (Springer, Wien, New York, 1990).

[41] A.I.Nachman, *Global uniqueness for a two-dimensional inverse boundary value problem*, Annals of Mathematics **143** (1996), 71-96.

[42] O.Scherzer, *The use of Tikhonov regularization in the identification of electrical conductivities from overdetermined boundary data*, Result. Math. **22**, No.1-2, 598-618 (1992)

[43] C.Schmeiser, *Voltage-current characteristics of multi-dimensional semiconductor devices*, Quarterly of Appl. Math. **4** (1991), 753-772.

[44] S.Selberherr, *Analysis and Simulation of Semiconductor Devices* (Springer, Wien, New York, 1984).

[45] T.I.Seidman, G.M.Troianiello, *Time-dependent solutions of a nonlinear system arising in semiconductor theory*, Nonlinear Analysis **9** (1985), 1137-1157.

[46] T.I.Seidman, C.R.Vogel, *Well posedness and convergence of some regularization methods for nonlinear ill posed problems*, Inverse Problems **5** (1989), 227-238.

[47] M.Stockinger , R.Strasser, R.Plasun, A.Wild, S.Selberherr, *A qualitative study on optimized MOSFET doping profiles*, Proc. of SISPAD 98 (Springer, 1998), 77-80.

[48] M.Stockinger , R.Strasser, R.Plasun, A.Wild, S.Selberherr, *Closed-loop MOSFET doping profile optimization for portable systems*, Proceedings Intl. Conf. on Modeling and Simulation of Microsystems, Semiconductors, Sensors, and Actuators (San Juan, 1999), 411-414.

[49] Z.Sun, *The inverse conductivity problem in two dimensions*, J. Differ. Equations **87** (1990), 227-255.

[50] J.Sylvester, G.Uhlmann, *A global uniqueness theorem for an inverse boundary value problem*, Ann. Math., II, **125** (1987), 153-169.

[51] W.R. Van Roosbroeck, *Theory of flow of electrons and holes in germanium and other semiconductors*, Bell Syst. Tech. J. **29** (1950), 560-607.